6-3-2015

Cell Wall Mutants in Arabidopsis Thaliana

Christy Jane Moore
Illinois State University, nickypuppys@gmail.com

CELL WALL MUTANTS IN *ARABIDOPSIS THALIANA*

Christy J. Moore

59 Pages August 2015

Plant cell walls are versatile structures, playing important roles in communication, defense, organization and support. The importance of each of these functions varies by cell type, with specialized cell walls often performing one or two functions more than others. *Arabidopsis* trichomes, or leaf hairs, and hypocotyl cells for instance, exhibit distinct cell wall characteristics. Trichomes of the *Arabidopsis* plant have developed very thick cell walls with several raised structures, known as papillae, on their surfaces. It is believed that these cells function in defense against predators, making it difficult to crawl on the leaf surface, and in protection against ultra violet radiation, through refraction of light via the papillae (1, 2, 3). Hypocotyl cells on the other hand are long and narrow, with cell walls that undergo extensive remodeling to permit rapid oriented cell growth (4). This enables hypocotyl cells to elongate along the axis of plant development, pushing the developing shoot through the soil.

To better understand the molecular processes important for papillae deposition on the cell wall surface, as well as for cell wall building and cell elongation, we focused on the identification and characterization of the *GLASSY HAIR (GLH)* and *SHORT HYPOCOTYL (SH)* genes, in which mutants display underdeveloped papillae and small dark-grown hypocotyls, respectively.

A candidate gene, *MED25*, located within the mapping region on chromosome 1, was identified for *glh1*. The gene was sequenced, revealing a point mutation in the splice junction of the sixth intron. A genetic complementation test was conducted, which showed that *MED25* was responsible for the *glh1* glassy phenotype. A mutant rescue via transformation with a genomic fragment including the *MED25* regulatory and coding regions was also performed, confirming gene identity. The genetic introduction of markers for trichome development *GLABRA2* (*GL2*) and *Ethylene Receptor2* (*ETR2*) into the mutant line demonstrated that the transcription of genes in trichomes is not generally changed in mutants. β-glucuronidase fusion with the promoter of the gene was also performed, confirming gene expression in trichomes.

The *glh2* and *glh3* mutations were rough mapped to chromosome 4 and 5, respectively. Genetic fine mapping was conducted to reduce the intervals in which the genes were thought to be located. Markers for trichome development were also introduced into each of these mutant lines to begin preliminary characterization of the nature of the mutations.

SH was rough mapped to a 2791kb region on chromosome 5. Known mutants within the mapping region that have *sh*-like phenotypes (*cobra* and *procuste1/cesa6*) were genetically or phenotypically tested to verify that *sh* was novel. A conditional radial expansion test revealed that *sh* does not exhibit a *cobra* phenotype. A confocal microscopy analysis of progeny from a *sh* x YFP-tagged CESA6 cross indicated that *SH* is not *CESA6* and that CESA6 appears to be sequestered in Golgi of *sh* plants. In addition, we measured birefringence, an optical property of crystalline cellulose, in mutant and wild type trichomes, revealing a possible cellulose deficiency. We performed

a biochemical cellulose assay to quantify the amount of cellulose in dark-grown mutant and wild type plants, to test this possibility.

CELL WALL MUTANTS IN *ARABIDOPSIS THALIANA*

CHRISTY J. MOORE

A Thesis Submitted in Partial
Fulfillment of the Requirements
for the Degree of

MASTER OF SCIENCE

School of Biological Sciences

ILLINOIS STATE UNIVERSITY

2015

CELL WALL MUTANTS IN *ARABIDOPSIS THALIANA*

CHRISTY J. MOORE

COMMITTEE MEMBERS:

Viktor Kirik, Chair

Martha Cook

John Sedbrook

ACKNOWLEDGMENTS

I would like to thank my research advisor, Dr. Viktor Kirik for his advice and support during my time here over the past two years at Illinois State University. I would especially like to recognize Dr. Kirik's patience and enthusiasm. It is easy to get discouraged when experiments fail or an unexpected hindrance is encountered time and time again, but he always remained positive, ready to push forward. I would also like to extend my gratitude to the rest of my committee members, Dr. Martha Cook and Dr. John Sedbrook, for their guidance and expertise. It has been a great learning experience, and I am confident that the knowledge and techniques that were passed onto me here will serve me well in the future.

The financial support provided to me through the duration of this program has been crucial to the completion of my research. For that reason, I would like to thank the School of Biological Sciences for the teaching assistantships awarded to me during the school year, and Dr. Kirik for proving support during the summer months. I would also like to show my appreciation to the Phi Sigma Biological Science Honors Society for Weigle Grant funding.

Last, but not least, I would like to thank my loving boyfriend, Kaleb, my friends, and family for providing me with endless support and advice throughout my time at ISU. A special thanks is also owed to my lab mate, Samantha Atkinson, and the Kirik lab

research coordinator, Dr. Angela Kirik, for their time, assistance, and kindness. My experience as a master's student was truly enriched by their knowledge and friendship.

C. J. M.

CONTENTS

FIGURES

Figure Page

CHAPTER I

INTRODUCTION

Arabidopsis as a Model Organism

Arabidopsis thaliana is a small flowering plant of the mustard family. Its small size and short life cycle of about six weeks, make *Arabidopsis* an ideal organism for laboratory work. In addition, *Arabidopsis* has a small genome, consisting of only five chromosomes, which has been completely sequenced (5, 6). The known sequence and gene information is available to the public on a web-based database, The Arabidopsis Information Resource, or TAIR (www.arabidopsis.org), facilitating the identification and characterization of novel phenotypes in this model organism.

The Plant Cell Wall

Plant cell walls are versatile structures, playing critical roles in communication, defense, growth and mechanical support. Their structure and strength are derived from the composition and interaction of component molecules, such as lignin and cross-linked polysaccharides (7). Their thickness and rigidity can serve as a physical barrier to protect the plant against predators, pathogens, and abiotic stressors (1). Oligosaccharins in the cell wall induce important cell signaling and defense pathways, ultimately regulating processes such as fruit ripening, production of defense chemicals,

and structural protein cross-linking (8). In addition, anisotropic cell wall expansion, a process by which cells elongate more in one direction over another, is largely responsible for plant growth and final organ size (9). While much is known about these various functions of the plant cell wall, there is still much left to learn concerning the processes of cell wall biogenesis, the deposition of materials on the cell wall surface, and oriented cell expansion.

Leaf Trichomes

Trichomes of the *Arabidopsis* plant are branched, single cell leaf hairs that exhibit thick cell walls with several raised, rounded structures, known as papillae, on their surfaces (Figure 1). It is believed that these cells may serve as physical obstacles on the leaf surface to discourage insect predation, as well as a sink for heavy metals, xenobiotics, and cytotoxins during detoxification and stress response processes (1, 10, 11). It has also been posited that trichomes and their papillae may refract incoming light to prevent water loss, increase drought resistance, and reduce the transmission of harmful Ultra Violet (UV) radiation onto the leaf surface (2, 3).

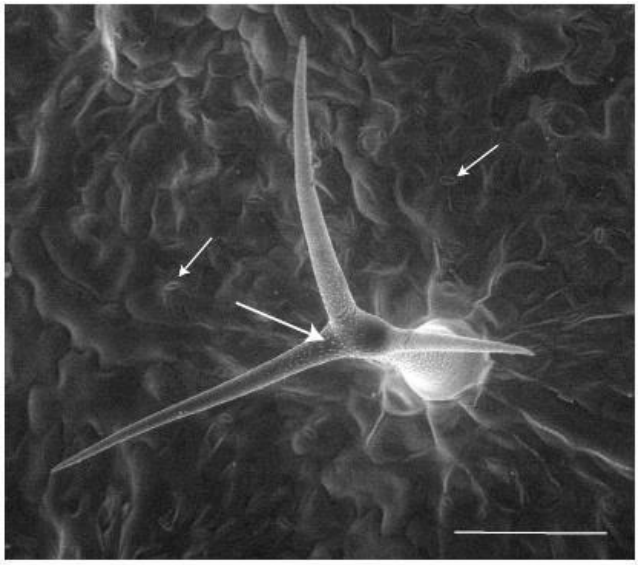

Figure 1 *Arabidopsis* Trichome
Papillae (bumps on trichome) indicated by large arrow. Stomata (pores) of leaf indicated by small arrows. Scale bar=100µm.

Certain cell wall mutants possess fewer, underdeveloped papillae, making their trichomes appear less "frosted" and more "glassy." The frosted appearance of wild type trichomes is believed to be caused by the uneven surface area created by papillae on the trichome cell wall. The curved structures are therefore proposed to scatter light in a similar manner as to that of frosted glass. When papillae are missing or less pronounced, this light scattering property is diminished and more light is permitted to pass through the trichome. The resultant "glassy" trichomes are distinguishable from wild type trichomes after the final stages of trichome maturation, during which papillae are formed (12).

glassy hair **Mutants**

One of my research projects focuses on the *glassy hair (glh)* mutants, *glh1, glh2* and *glh3*. The *glassy hair* mutants possess trichomes that have a low density of underdeveloped papillae on their cell wall surfaces, causing them to appear "glassy" rather than "frosted" (Figure 2). Of the three mutants, *glh2* exhibits the glassiest trichomes, corresponding to the severity of underdevelopment and scarcity of papillae. The *glh1* mutant has a slightly less glassy trichome phenotype, which is also due to a reduced size and density of papillae. The *glh3* mutant on the other hand, exhibits an intermediate trichome phenotype that is less glassy than those of the previous two mutants but more glassy than that of wild type. This mutation is caused by the presence of a low density of more fully developed papillae.

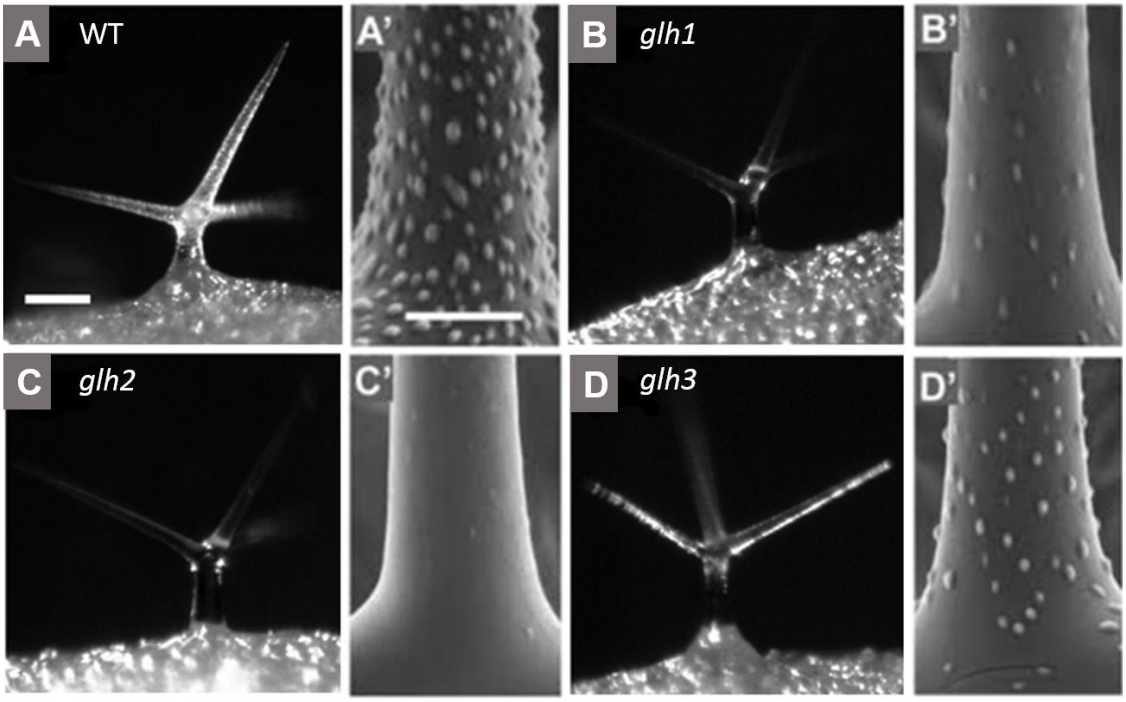

Figure 2 *glh* Mutant Trichomes

Wild type trichomes appear frosted (A) and have fully developed papillae at high a density (A'). Mutant trichomes appear glassy (B-D) and have underdeveloped papillae at a low density (B'-D'). Polarized light images, scale bar=100μm (A-D). Scanning electron microscope images, scale bar=20μm (A'-D'). Images reproduced with permission from Suo *et al* 2013 (12).

Hypocotyl Cells

Arabidopsis hypocotyl cells, are long, narrow cells that elongate along the axis of plant growth, pushing the developing shoot through the soil (Figure 3). This is accomplished through a biphasic process involving an initial phase of cellulose deposition in the cell wall and slow growth, and a subsequent phase of substantial cell wall polysaccharide remodeling and rapid growth (4). Together, these two processes enable young seedlings to perform anisotropic cell growth.

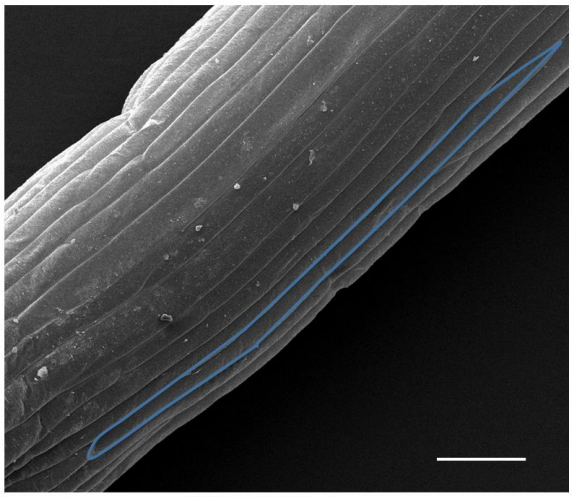

Figure 3 Hypocotyl Cells
Hypocotyl cells are long and narrow in shape, and elongate along the axis of plant growth. The perimeter of one cell is outlined in blue. Scale bar=50µm.

Certain cell wall mutants are deficient in the process of elongation, causing their hypocotyls to be swollen and shorter than those of wild type plants (13-17). This difference is most noticeable when these mutants are grown in darkness. This is due to the nature of seedlings; young plants that have yet to be exposed to light will elongate until the darkness barrier is broken and sunlight is encountered. A longer period of time spent in darkness consequently corresponds to a longer period of time elongating.

***short hypocotyl* Mutant**

My other research project focuses on the *short hypocotyl (sh)* mutant. This mutant exhibits a smaller and slightly swollen hypocotyl in comparison to wild type when grown in darkness for five to six nights (Figure 4). Mutant plants retain their smaller stature

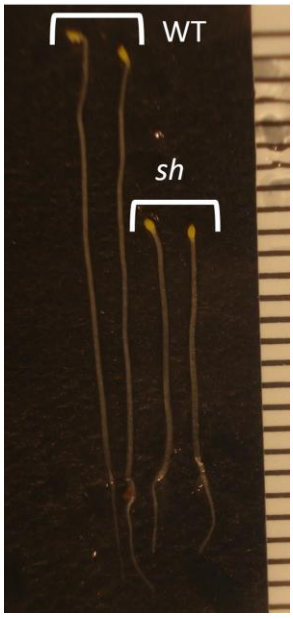

Figure 4 *short hypocotyl* Phenotype
The hypocotyls of six-day-old, dark-grown, *short hypocotyl (sh)* plants are much shorter and slightly thicker than those of wild type (wt) plants of the same age and grown under the same conditions. Each mark of the ruler represents 1mm.

into maturity, though the difference becomes less pronounced.

Significance

The *Arabidopsis* leaf trichome represents an excellent model for studying the mechanisms of cell wall development. While several genetic mutations may cause a glassy trichome phenotype, the identity and molecular function of many of these genes have yet to be elucidated (12, 18, 19). Such knowledge would provide insight into, not only the function of each specific gene, but also the cellular processes important for the focused deposition of cell wall material at large.

Similarly, though several cell wall mutations have been identified that result in short hypocotyl cells, most of these mutations affect distinct players involved in the processes of cell wall building and cell elongation (13-17). This suggests a complex interaction of molecular and cellular processes that ultimately leads to the production of a normal hypocotyl phenotype. Identifying and characterizing the genes that cause defects in hypocotyl elongation would therefore allow us to better understand not only the specific function of each of these genes, but also the complex processes of cell wall biogenesis and oriented cell expansion in general.

CHAPTER II

METHODS

Plant Growth Conditions

For plants that needed to be aseptically grown, plates containing one half Murashige and Skoog (MS) salt and varying amounts of sucrose and 2-(N-morpholino)ethanesulfonic acid (MES) were used. Those plates used for growing *short hypocotyl* mapping population plants contained 1% sucrose and 50mg MES. Plates used for the conditional radial expansion test contained 50mg MES and either 0.1% or 4.5% sucrose. Those used to grow T1 seeds contained 50mg MES, 1% sucrose, and an antibiotic for selective purposes. All plates were placed in a 4^{o}C refrigerator for two nights to break seed dormancy. Afterwards, *short hypocotyl* mapping and conditional radial expansion test plates were grown vertically, in darkness, and at room temperature for four to six nights. T1 plates were grown at 22^{o}C in a growth chamber for approximately ten days.

A soil mixture consisting of one half Promix with mycorrhizae and one half Professional Growing Mix was used for plants grown in pots. One tablespoon of Osmocote plant food was added to each tray of pots to supplement plant growth. Seeds were distributed onto pots of wet soil. Trays were then covered and placed in a 4^{o}C cold room for two nights to break seed dormancy. Afterwards, trays were placed in the green house and plants were grown at room temperature. Covers were removed after plants

were strong enough to withstand lower humidity levels. Mature plants were supported with bamboo stakes.

Seed Sterilization

Seeds meant to be grown on plates were aseptically sterilized in a laminar flow hood. Seeds were first placed into 1.5ml microfuge tubes, with approximately ten to fifteen seeds per tube. Then, 500µl of 70% ethanol (ETOH) was added to each tube and allowed to stand for at least one minute, but not longer than two minutes. The ETOH was decanted, and 800µl of double-distilled water (ddH2O) was added to each tube. Tubes were mixed by inversion and spun in a microcentrifuge until a speed of 6,000rpm was reached. The ddH2O was decanted and 800µl more of ddH2O was added to the tubes, mixed by inversion, and left to stand for five minutes. The tubes were again spun in a microcentrifuge until it reached a speed of 6,000rpm. Then the ddH2O was decanted, and 800µl more of ddH2O was added to each tube. Seeds were then either transferred directly to plates or stored in the 4^{o}C refrigerator until needed for plating.

Transformation T1 seeds were also aseptically sterilized in a laminar flow hood, however the protocol differs slightly from above. Seeds were placed into 2ml microfuge tubes with approximately 200 seeds per tube. Then, 500µl of 70% ethanol (ETOH) was added to each tube and allowed to stand for at least one minute, but not longer than two minutes. The ETOH was decanted, and 1ml of a one-to-one bleach and deionized water solution was added to each tube. The seeds were allowed to stand in this solution for five minutes prior to being centrifuged at 6,000rpm for fifteen seconds. Then, 800µl of double-distilled water (ddH2O) was added to each tube. Tubes were mixed by

inversion and spun in a microcentrifuge at 6,000rpm for fifteen seconds. The ddH2O was decanted and 800µl more of ddH2O was added to the tubes, mixed by inversion, and left to stand for five minutes. The tubes were again spun at 6,000rpm for fifteen seconds. Then the ddH2O was decanted, and 800µl more of ddH2O was added to each tube. Seeds were then either transferred directly to plates or stored in the 4°C refrigerator until needed for plating.

Seeds meant to grown in soil were sterilized by placing the seed bags in the -80°C freezer overnight prior to planting. This method was employed primarily to kill any thrips eggs; thrips are insects that feed on the cell contents of leaves and flowers, and as a result, stunt plant growth.

DNA Isolation

For each plant, two to three leaves were harvested, placed in a 1.5ml microfuge tube, and stored in a -80°C freezer. When DNA was to be isolated, the tubes were removed from storage at -80°C and placed in liquid nitrogen. Large forceps were used to remove a tube from the liquid nitrogen container. A pestle was then dipped in the liquid nitrogen for approximately five seconds and subsequently used to vigorously grind up the leaves. As soon as the leaves began to warm, 500µl of extraction buffer was added and the tube was left to stand. This process was repeated for two additional tubes, with a new pestle used for each sample. Starting with the first tube and finishing with the third, leaves were then ground again and put on ice. The grinding process was subsequently repeated until all samples were on ice. Afterwards, the tubes were all mixed by inversion and incubated at 65°C for twenty minutes.

Once the incubation was complete, the samples were taken to the fume hood where 500µl of a chloroform: iso-amyl alcohol mix (24:1) was added to each tube. The tubes were mixed by inversion and spun in a microcentrifuge at 12,000rpm for ten minutes. Tubes were subsequently put on ice and for each sample, approximately 400µl of the clear supernatant was transferred to a new 1.5ml microfuge tube. (The remaining solution for each sample was discarded into the appropriate waste container in the fume hood.) Then 1ml of cold 95% ETOH was added to each tube, and the tubes mixed by inversion until strings of DNA were visible. The samples were spun at 12,000rpm for fifteen minutes and then put on ice. Double tips were used to discard the supernatant and then 400µl of cold 70% ETOH was added to each tube. The samples were spun at 12,000rpm for two minutes and put back on ice. Double tips were used to discard the supernatant and the tubes were left open to dry for about fifteen minutes. The pellets were then re-suspended in 30-50µl of ddH2O, depending on the size of the pellet.

The extraction buffer was a 1:1 mix (made directly before use) of two sterile buffers. Buffer #1 consisted of 31.9g of 0.35M sorbitol, 6.05g of 0.1M tris(hydroxymethyl)aminomethane (Tris), 0.95g 5mM ethylenediaminetetraacetic acid disodium salt (EDTA-Na2), and ddH2O up to 0.5L. The pH was adjusted to 8.25 with hydrochloric acid (HCl). Buffer #2 consisted of 100ml of 200mM Tris, pH 8.0, 50ml of 50mM ethylenediaminetetraacetic acid (EDTA), pH 8.0, 10g 2% cetyl trimethylammonium bromide (CTAB, which was first diluted separately in water and then added to buffer #2), and ddH2O up to 0.5L. To calculate how much buffer to use for a certain sample size, the following formula was used: (.5xsample size) +1ml. 1ml was added to make sure enough buffer was present for pipetting.

Bulked Segregant Analysis

Columbia ecotype mutants were crossed to Landsberg erecta ecotype plants. F2 seeds were grown and tissue samples of mutants were harvested. Genomic DNA was isolated from these mapping population samples. A pooled DNA sample of the mapping population was created by mixing 1µl from 39 individual samples together in a separate tube. Three simple sequence length polymorphism (SSLP) makers were selected, one from the upper arm, one from the middle, and one from the lower arm, for each of the five *Arabidopsis* chromosomes and used to design polymerase chain reaction (PCR) primers. PCR was performed on the pooled mapping population DNA mixture as well as a Columbia-Landsberg erecta DNA mixture using each of the selected primers, and the reactions were subsequently run out on an agarose gel. The Columbia-Landsberg erecta DNA mixture served as a heterozygous control, against which the band(s) of the mapping population mixture may be compared. The pooled mapping population sample was homozygous Columbia for markers near the mutation site, but heterozygous (both Columbia and Landsberg erecta) for all other unlinked loci. Therefore, the chromosome on which the mutation of interest resided was identified through the detection of markers for which the mapping population sample was of a Columbia background instead of heterozygous (20).

Genetic Rough Mapping

Columbia ecotype mutants were crossed to Landsberg erecta ecotype plants. F2 seeds were grown and tissue samples of mutants were harvested. Genomic DNA was

isolated from these mapping population samples. Three SSLP makers were selected, one from the upper arm, one from the middle, and one from the lower arm, for each of the five *Arabidopsis* chromosomes and used to design PCR primers. PCR was run on twenty of the mapping population samples using each of the selected primers, and the reactions were run out on an agarose gel. The number of plants that were of a Columbia, Landsberg erecta, or heterozygous (both Columbia and Landsberg erecta) background for each of the markers was scored and analyzed. The larger the number of plants that were of a Columbia background for any given marker, the closer the mutation of interest was located to that marker. This enabled the identification of both the chromosome and the general region on the chromosome that held the mutation of interest. Additional markers and mapping population samples were used to pursue further mapping, and as plants that were heterozygous at previous markers became Columbia at new markers, the mapping region became more defined (20).

Genetic Fine Mapping

Columbia ecotype mutants were crossed to Landsberg erecta ecotype plants. The F2 seeds were grown and tissue samples of mutants were harvested. Genomic DNA was isolated from these mapping population samples, and SSLP, cleaved amplified polymorphism (CAP) or derived CAP (dCAP) markers were used for PCR amplification. PCR reactions were run out on an agarose gel and recombinants (heterozygotes) were counted. The fewer recombinants found for a marker, the closer that marker was to the gene of interest. Once approximately ten recombinants were found for the current set of markers, new markers located further inward in the mapping interval were selected for

testing those samples. As recombinants were lost (the samples became Columbia at the new markers), additional mapping population samples were tested (20). This process was repeated until the mapping interval was less than 100kb and nearly all recombinants were lost.

T-DNA Line Selection and Screening

Once a fine mapping interval of less than 100kb was reached, the web-based database TAIR (www.arabidopsis.org), was used to look for transfer DNA (T-DNA) lines located within that region. T-DNA lines were selected based on the known functions of their interrupted genes; those involved with processes likely or possibly involved in the production of the observable phenotype of interest were ordered first. The selected T-DNA lines were then grown on soil and screened for the mutant phenotype once they had reached the appropriate developmental stage. If a T-DNA line was found that exhibited the mutant phenotype, the interrupted gene was considered a candidate for the gene of interest.

Sequencing

Candidate genes were sequenced along with a wild type control to find the site of mutation using dye-terminator Sanger sequencing techniques. A 5µl reaction mixture consisting of 1µl BigDye Terminator v1.1/3.1 Sequencing Buffer (5X), 0.5µl BigDye Ready Reaction Mix, 0.2µl 10µM primer, 12.5-37.5ng DNA template, and ddH2O to bring the total volume up to 5µl. The amount of DNA used varied depending on the type and length of the template to be sequenced. The reaction was mixed thoroughly and

placed in a thermocycler that executed the following conditions: 94°C for two minutes, followed by forty cycles of a ten second denaturation step at 96°C, a twenty second annealing step at 52°C, and a three and a half minute extension step at 60°C. An ethanol precipitation was then carried out on the sequencing reaction to precipitate the DNA out of solution. To this end, 15µl ddH2O were added to the reaction, followed by 0.5µl 0.5M EDTA, 2µl 3M sodium acetate (NaAc), and 50µl 100% ETOH. The sample was incubated at -20°C for twenty minutes, and then spun at 12000rpm and 4°C for thirty minutes. After, the sample was washed with 300µl cold (-20°C) 70% ETOH and pulse centrifuged at 4°C. The pellet was air dried and sent to the on-site sequencing facility. There, the DNA fragments were separated out by capillary gel electrophoresis, fluorescent peaks were detected, and a chromatogram was constructed.

PCR Cleanup

Prior to sequencing, deoxynucleotide triphosphates (dNTPs) and primers were removed from PCR products using the Nucleics ExoSAP protocol (www.nucleics.com). A master mix was prepared consisting of 1µl FastAp alkaline phosphatase (Fermentas, 1u/µl) and 0.5µl Exonuclease I (New England Biolabs, 20u/µl) per PCR product. Then, 1µl of this master mix was added to 5µl of each PCR product, and the reactions were placed in a thermocycler that executed the following conditions: 37°C for fifteen minutes, followed by 85°C for fifteen minutes.

Genetic Crosses

Plants to be used in genetic crosses were grown as previously described. Once the plants began flowering, approximately two to three buds from each genetic line were emasculated to prevent self-fertilization. To accomplish this, both the sepals and the petals were carefully detached prior to removing the stamens, the male sex organs. Each bud was then left with only a pistil, the female sex organ. Once the pistils of one genetic line reached sexual maturity, characterized by an open and extended stigma, they were manually pollinated by removing an open flower from the other genetic line and gently brushing its anthers over the open stigma. Successful pollination events resulted in elongated siliques (seed pods), which were dry harvested upon maturation. Silica crystals were used to dehydrate seeds obtained from each cross for two days post collection.

Gel Extraction

Prior to molecular cloning, primers, enzyme, and unincorporated nucleotides were removed through gel extraction. The DNA sample to be used as an insert was run out on an agarose gel. The gel was placed on an Ultra Violet (UV) light box and the fragment intended to be cloned was excised using a razor blade. The DNA fragment was subsequently isolated and purified using the Gene Jet PCR Purification Kit produced by Fermentas. Briefly, the weight of the excised gel slice was determined, and a one-to-one amount of binding buffer was added to the tube. The sample was then heated at 50^{o}C for ten minutes to dissolve the gel fragment. Next, 800µl of the sample was added to a GeneJET purification column, which was placed inside a collection tube and spun at 12,000rpm for one minute. The flow-through was discarded, 700µl of wash buffer was

added, and the column was spun at 12,000rpm for one minute. The flow-through was discarded and the empty column was spun at 12,000rpm for one more minute to remove any remaining wash buffer. The column was subsequently transferred to a clean 1.5ml microfuge tube, and 50µl of warm (65°C) elution buffer was added to the middle of the column. After a one minute incubation at room temperature, the column was spun at 12,000rpm for thirty seconds to elute the DNA. The DNA was stored at -20°C.

A-Tailing and pCR8 Cloning

The DNA concentrations of the gel purified insert were measured using a spectrophotometer. Concentrations ranging from 1.3-13ng/µl were used for cloning to determine optimal conditions. A 3.5µl sample of the insert was mixed with 0.5µl 10x Taq polymerase buffer, 0.5µl 2mM deoxyadenosine triphosphate (dATP), and 0.5µl Taq polymerase enzyme. The reaction was then incubated at 72°C for thirty minutes. After the incubation was complete, 2.1µl of the reaction product was added to a mixture of 0.5µl salt solution and 0.4µl pCR8/GW/TOPO vector. The cloning reaction was incubated at room temperature overnight.

Gateway LR Cloning

The DNA concentrations of the entry clone (pCR8/GW/TOPO containing the insert) and the destination vector (pMDC162) were measured using a spectrophotometer. Concentrations ranging from 12.5-40ng/µl were used for cloning to determine optimal conditions. A 0.5µl sample of entry clone was added to a mixture of 1µl Tris-EDTA (TE) buffer, pH 8.0, and 0.5µl destination vector. Then, 0.5µl of the LR Clonase enzyme was

added, and the reaction was mixed well by pipetting up and down slowly. The reaction was incubated at room temperature overnight.

Electro-Competent Bacteria Transformation

Dialysis was performed on DNA constructs prior to transformation into electro-competent *Escherichia coli (E. coli)* cells to remove salts. The bottom a small petri dish was covered with ddH2O, atop of which a one fourth piece of Millipore membrane filter was floated. The desired amount of DNA construct (usually 1-3µl) was pipetted onto the membrane and allowed to sit for twenty minutes.

After dialysis of the construct was complete, a 50µl aliquot of either electro-competent *E. coli* or agrobacteria cells was put on ice to thaw and a 1mm cuvette was placed on ice to chill. The competent cells and 1µl of construct were combined and gently mixed. The mixture was pipetted into the cold cuvette, which was then tapped to ensure even distribution of the liquid between the electrode plates. The 1mm cuvette, 1700voltz setting was selected on the electroporator and the cuvette was dried, placed in the machine, and the shock was initiated. Once the shock was complete, 500µl of Super Optimal broth with Catabolic repressor (SOC) medium for *E. coli*, or Yeast Extract Broth (YEB) medium for agrobacteria, was added into the cuvette and mixed at room temperature. The total volume was then pipetted into a 1.5ml microfuge tube and shook at 850rpm according to the type of competent cells. In *E. coli* transformations, the tube was shook at 37^{o}C for forty five minutes to an hour; in agrobacteria transformations, the tube was shook at 28^{o}C for one to two hours.

After shaking, the tube was taken to a sterile flow hood where 50µl of bacterial suspension was spread onto a nutrient plate. Luria broth (LB) plates were used for *E. coli* cells while YEB plates were used for agrobacteria cells. Each nutrient plate contained the appropriate antibiotics to select for successful transformants. The remaining cells were spun down at 6,000rpm for thirty seconds, and all but approximately 100µl of the supernatant was decanted. The tube was taken back to the flow hood, and the pellet was re-suspended. The rest of the bacterial suspension was spread onto a second nutrient plate. Both plates were then incubated upside down in an oven. The temperature and duration of the incubation varied with type of transformation. Plates from an *E. coli* transformation were incubated at 37^{o}C overnight. Plates from an agrobacteria transformation were incubated at 28^{o}C for two to three days, after the first of which, the plates were wrapped with parafilm to prevent dehydration. Afterwards, all plates were stored at 4^{o}C until no longer needed.

Plasmid Isolation

Bacterial plasmids were isolated from liquid cell culture using the Zyppy Plasmid Mminiprep Kit by Zymo. Briefly, 1,500µl liquid bacterial culture was transferred to a 1.5ml microfuge tube and spun down at maximum speed for thirty seconds. The supernatant was discarded and approximately 1,400µl more liquid bacterial culture was added to the tube. The tube was spun down at maximum speed for thirty seconds, the supernatant was decanted, and the pellet was re-suspended in 600µl ddH2O. Next, 100µl of 7x lysis buffer was added and the tube was mixed via inversion until the sample changed from opaque to clear. Within two minutes of adding the lysis buffer,

350µl cold (4°C) neutralization buffer was added to halt the reaction. The tube was mixed by inversion until a yellow precipitate formed, and then it was centrifuged at 14,000 x gravity (g) for three minutes. Approximately 900µl of the supernatant was transferred to a Zymo-Spin IIN column, which was placed inside a collection tube and spun at 14,000 x g for fifteen seconds. The flow-through was discarded, 200µl endotoxin wash buffer was added, and the column was centrifuged at 14,000 x g for thirty seconds. Then, 400µl Zyppy wash buffer was added and the column was spun at 14,000 x g for one minute. The column was subsequently transferred to a clean 1.5ml microfuge tube and 30µl Zyppy elution buffer was added to the middle of the column to elute the plasmid DNA. After a one minute incubation at room temperature, the column was spun at 14,000 x g for thirty seconds to elute the DNA. The DNA was stored at -20°C.

Restriction Digest Analysis

Either 2µl plasmid DNA or 4µl PCR product was added to 1µl of the appropriate restriction enzyme buffer, 0.3µl of each desired restriction enzyme, and ddH2O up to 10µl. The reaction was incubated at 37°C for one hour, and then analyzed by gel electrophoresis. Restriction enzymes were chosen based on known cut sites in the plasmid or PCR product. Expected band sizes were calculated based on the cut sites and sizes of the resultant pieces.

Plant Transformation

First, 100ml YEB medium was poured into an Erlenmeyer flask inside a laminar flow hood. The appropriate antibiotics to select for successful transformants were

added to the medium. Sterile forceps were used to pick up a sterile p100 pipette tip, which was then dipped into a glycerol culture containing agrobacteria transformed with the construct of interest. A chunk of frozen culture approximately the size of two to three grains of rice was removed and dropped into the YEB medium. The Erlenmeyer flask was then covered with foil and incubated at 28^{o}C in a shaking incubator for two nights.

After two nights, the liquid bacterial culture was placed in a centrifuge tube and weighed for balancing purposes. The culture was spun at 4,000rpm for ten minutes at room temperature. Infiltration medium consisting of 5% sucrose and 0.05% sillwett 77 was prepared by mixing 10g sucrose, 100µl sillwett, and 200ml deionized water in a beaker. The supernatant was discarded, the pellet was re-suspended in the infiltration medium, and the solution was poured into a beaker. Pots of Arabidopsis plants (usually about six pots containing six plants each) were prepared for the transformation by pushing down on the soil to prevent lose plants and soil from dislodging. The pots were then turned upside down and dipped into the infiltration-cell solution for twenty seconds. Afterward, each pot was laid on its side in a moist tray. To retain moisture, paper towels were sprayed with water until damp, and then placed along each side of the tray. Once all of the pots had been dipped, the tray was covered for twenty four hours. Then the cover was removed, the pots were stood upright, and the tray was placed in the greenhouse.

GUS Staining

A total volume of 100µl β-glucglucuronidase (GUS) staining solution was used when staining extremely young leaves (leaves that only measured a few millimeters in length). A total volume of 325µl GUS staining solution was used when staining young

seedlings (approximately 10-14 days old). The GUS staining solution was prepared as described in Xu and Li 2011 (21), and consisted of 40µl/ml 1mM 5-bromo-4-chloro-3-indolyl-beta-D-glucuronic acid, cyclohexylammonium salt (X-Gluc) diluted in GUS staining buffer. The GUS staining buffer was prepared using 50mM sodium phosphate buffer (pH 7.0), 0.4mM K3Fe(CN)6, 0.4mM K4Fe(CN)6, and 0.1% (v/v) Triton X-100. To calculate the amount to X-Gluc and staining buffer needed, the total volume required was first determined. This volume was used to calculate the amount of X-Gluc required. This number was then subtracted from the total volume to give the necessary amount of staining buffer. See below for example calculations. The samples were incubated at 37°C overnight. Afterward, the GUS staining solution was removed and 70% ETOH was added to remove chlorophyll and preserve the samples.

Samples were imaged using a Leica CCD camera and both a dissecting scope and a light microscope. Dissecting scope images were taken using the 6.3x, 10x, 16x, 20x, 32x, and 60x objectives with 600mm exposure. Light microscope images were taken using the 10x and 20x objectives. A numerical aperture of 2 and an exposure of 560µµ was used for the images taken with the 10x objective. A numerical aperture of 3 and an exposure of 1mm 750µµ was used for images taken with the 20x objective.

sh Phenotype Analysis

Columbia ecotype *glh3* mutants were crossed to Landsberg erecta ecotype plants. The *sh* mutant was found segregating out of the F2 generation of this mapping population. To select for *sh* plants, approximately two hundred F2 seeds were aseptically sterilized and spread in straight lines across MS 1% sucrose plates. Wild type Columbia

seeds as well as *sh* x YFP-CESA F2 seeds (F1 plants were selected for *sh* phenotype) were also sterilized and plated in a similar manner to serve as control plants. The plates were double sealed with medical tape and incubated at 4°C for two nights to break seed dormancy. Afterwards, the plates were wrapped in foil to prevent light from reaching the seedlings, situated vertically so that the seedling would elongate parallel to the surface of the agar, and incubated at room temperature for five nights.

Once the incubation period was over, the plates were unwrapped and phenotypically analyzed. The mapping population plates were screened for plants with etiolated hypocotyls as short as, or shorter than, those of the *sh* x YFP-CESA control plants. Any plants that exhibited an etiolated hypocotyl as tall as the Columbia control or of intermediate height were discarded. The plates were then taped back up and the plants were allowed to grow in light conditions at 22°C for two days. Upon which time, the plants were large enough to be transferred to soil. After approximately three weeks, tissue samples were harvested in duplicate from each plant and stored at -80°C. In addition, seeds were collected from each of the plants once their siliques had dried.

The *sh* phenotype of each of the plants selected for in the first screen was verified by phenotypically analyzing each line in the next generation. Approximately ten to fifteen seeds from each plant were aseptically sterilized and spread in straight lines across MS 1% sucrose plates. Columbia and *sh* x YFP-CESA F2 seeds were also sterilized and plated to serve as controls. The plates were incubated in the same manner as described above. Afterwards, each line was examined to ensure a clear and consistent *sh* phenotype was seen amongst the progeny. If plants with wild type length or

intermediate length etiolated hypocotyls were found for any given line, then the tissue harvested from the parent plant was excluded from use in genetic mapping procedures.

Conditional Radial Expansion Test

This experiment was based off of tests performed in Roudier *et al* 2005 (17). Columbia, Landsberg erecta, and *short hypocotyl* seeds were aseptically sterilized and plated on two sets of 0.1% and 4.5% sucrose MS plates. One set of plates was grown in darkness, and one was grown in light. All plates were grown vertically for six days at 22^{o}C. On day six mutant plants were analyzed for a conditional radial expansion phenotype (i.e. swollen, radial expanding roots and hypocotyl and thick cotyledons).

Trichome Isolation

Trichomes were isolated as described in Marks *et al* 2008 (22). Plants were grown in soil as described above. To ensure that the samples were all of the same developmental stage, only fully expanded rosette leaves of plants that began to form flower buds were harvested for trichome isolation. Approximately 1.5g of leaf tissue was added to a 50ml centrifuge tube along with approximately 50mg 60/80µm glass beads and 15ml of a 50mM ethylene glycol tetraacetic acid (EGTA), pH 7.5, and a 1x modified phosphate-buffered saline (PBS) solution. The modified PBS was made with only potassium salts. The centrifuge tube was then subjected to four cycles of vortexing at maximum speed for thirty seconds followed by thirty seconds on ice. The contents of the tube were then strained through several layers of wire mesh. PBS was used to rinse the cell material and free trapped trichomes. The solution that passed through the mesh was

then filtered through a 100µm cell strainer. The contents of the strainer were poured into a Petri dish and the strainer was rinsed several times with a total of 10ml PBS to dislodge any wedged trichomes. The resulting solution was transferred to a 15ml centrifuge tube and spun at 150xg for one minute, thirty seconds. The supernatant was removed and the pellet was re-suspended in approximately 25µl PBS. Then, 5µl was removed and used for cell counting. Six cell counts were averaged together to determine approximate trichome concentration. Approximately two thousand trichomes were aliquoted for UV absorption analysis and cellulose quantification.

UV Absorption Test

Triplicate aliquots of two thousand Columbia trichomes as well as two thousand mutant trichomes, each in 100µl PBS, were pipetted into a 96well UV microplate. Triplicate wells containing 100µl of PBS were used as blanks. The plate was read at 297nm and 357nm to measure UV-B (range 280nm-315nm) and UV-A (range 315-400nm) absorption, respectively. The triplicate readings were averaged and analyzed using a two-tailed t-test to determine if there was a statistical difference between the absorptive properties of wild type and mutant trichomes in regard to UV light.

Cellulose Quantification

Cellulose was quantified in seedlings and trichomes using an anthrone colorimetric assay developed by Updegraff 1969 (23) and modified by Gillmor *et al* 2002 (24). Groups of ten Arabidopsis seedlings, or two thousand trichomes, were placed into

1.5ml microfuge tubes. The samples were incubated in 1ml 70% ETOH at 70°C for one hour, followed by a forty five minute incubation in 1ml fresh ETOH at the same temperature. The ETOH was removed and 1ml acetone was added. The samples were incubated for 10 minutes at room temperature, after which they were left to dry overnight.

The next day, the weight of the dried tissue in each tube was recorded. Then 1ml acetic-nitric reagent was added and the tubes were placed in a boiling water bath for thirty minutes. The samples were spun down at 14,000rpm for ten minutes and the supernatant was carefully removed. Then 1ml ddH20 was added and the tubes were inverted prior to centrifugation at 14,000rpm for ten minutes. Half of the supernatant was removed and 1ml acetone was added. The tubes were spun at 14,000rpm for five minutes, and subsequently 1ml of the supernatant was removed. An additional 1ml acetone was added, again followed by centrifugation at 14,000rpm for five minutes. As much supernatant as possible was carefully removed and the remaining cell wall material was left to dry overnight.

The next day, 100µl 67% H2SO4 was added and the samples were vortexed thoroughly. Next, 400µl ddH2O and 1ml cold (4°C) anthrone solution were added to the tubes while on ice. The tubes were then transferred to a boiling water bath for five minutes. The samples were transferred back on ice for five minutes to stop the reaction. After the samples cooled to room temperature, the absorbance of each of the final solutions was measured using a spectrophotometer and a plate reader at 620nm.

A 10mM glucose stock solution was used to prepare triplicates of 0.1M, 0.2M, 0.3M, 0.4M, 0.6M, and 0.8M standard solutions. Then 1ml anthrone reagent was added

to each standard and the tubes were boiled and iced as noted above. The average absorbance of each triplicate of known concentration was used to construct a standard curve by which the concentrations of the unknowns were determined.

The anthrone reagent was made fresh daily by mixing 100mg anthrone with 10ml concentrated sulfuric acid. The solution was chilled for at least two hours prior to use. The acetic nitric reagent was prepared by adding 150ml 80% acetic acid to 15ml concentrated nitric acid.

Birefringence Analysis

Leaves three and four from four week old wild type Columbia and *short hypocotyl* plants were fixed via two different methods in parallel. The methanol/lactic acid method was conducted as described in Bischoff *et al* 2010 (25). Briefly, the leaves were first incubated in 300µl methanol for twenty minutes to remove cuticular waxes and eliminate potential interference with the birefringence caused by crystalline structures. Then they were boiled in 200µl 85% lactic acid for one hour. Afterward, the leaves were washed three times with water. In the formaldehyde-acetic acid method, the fixative was prepared by mixing 95% ETOH, 30-40% formaldehyde, acetic acid, and ddH2O in a 50:10:5:35 ratio. (The ethanol in this solution served the same purpose as the methanol in the previous method.) The leaves were incubated in approximately 500µl of the fixative for six to twelve hours at 4^{o}C.

The trichomes of the fixed leaves were viewed using polarized light microscopy and the 20x objective at a 360mm exposure time. The microscope stage was rotated to achieve the maximum birefringence of one branch of each trichome examined,

and the Lieca CCD camera was used to take images once maximum birefringence was achieved. Approximately twenty images were taken for each plant line-fixation method combination. ImageJ software was subsequently used to measure the average light intensity of the birefringent branch for each trichome imaged. First, background values at a rolling ball radius of 50 pixels were subtracted from each image. Next, the freehand tool was used to draw a box around the middle section of the birefringent branch. Then the average light intensity of this area was measured. The area of the box was kept consistent between branches. A two-tailed T-test was used to determine of there was a statistical difference between the average light intensity of wild type and mutant images.

Confocal Microscopy

Spinning disc confocal microscopy was used to image Yellow Fluorescent Protein (YFP)-Cellulose Synthase (CESA) signal in the etiolated hypocotyls of five day old wild type Columbia and mutant seedlings. Seeds were sterilized and plants were grown as described in the *SH* Phenotype Analysis section. On day five, the plates were unwrapped and plants were viewed using a 100x oil immersion objective and the 488nm laser. The parameters in the Focus window were set as follows: neutral density of 14, disc speed of 2,000, exposure time of 250ms, and intensification of 180. For time lapse images, the Capture window parameters included a six second interval, with twenty time points, and an exposure time of 600ms. For Z-stack images, the Focus window parameters outlined above were used and in addition, the stack depth was set to begin at the cell wall plane and end 3µm into the cell. The Capture window settings for these 3D images included six planes, a 0.5µm step size, and an exposure time of 500ms. Time

lapse images of both the fifth cell down from the hook, as well as a cell directly from the middle of the hypocotyl were taken. Z-stack images were taken only of the fifth cell down from the hook.

The density of YFP-CESA particles in wild type and mutant cells was determined using ImageJ software according to the protocol described in Bashline *et al* 2013 (26). First, a time lapse image was opened and screened for a good resolution, in-focus frame that included the plasma membrane plane. The selected frame was separated from the stack for processing and analysis. The frame was rotated so that the cells were in a vertical position, and the image was cropped so that just the cell of interest was included. Next, the contrast was enhanced to 0.4% pixel saturation, and background values with a rolling ball radius of 15 pixels were subtracted. A region of interest (ROI) was selected, excluding any areas exhibiting Golgi signal from the cytosolic plane. The Find Maxima function was used to detect the number of particles present in the selection, and an identical noise tolerance of 1,400 was used for all analyses. The measure function was used to determine the area of the selection in μm^2. Finally, the number of particles was divided by the area to give the particle density for the cell. A two-tailed T-test was used to determine if the particle densities of wild type and mutant cells were statistically different.

Scanning Electron Microscopy

Plant tissue was prepared for microscopy via primary fixation in a 4% glutaraldehyde-phosphate buffer solution. After two hours, the primary fixative was removed and the plant tissue was rinsed three times with phosphate buffer, with ten

minutes per wash. A secondary fixation was carried out using a 1% osmium tetroxide-phosphate buffer solution. The secondary fixative was removed after one hour and the plant tissue was rinsed as before. Samples were then dehydrated via ten minute incubations in increasing concentrations of ETOH that were performed as follows: 10%, 30%, 50%, 70%, 95%, 100%, 100%, 100%. After, critical point drying was carried out for one hour. Finally, the samples were mounted on stubs and sputter coated with gold.

SEM images were taken as described in Suo *et al* 2013 (12). Trichomes of three week old plants were viewed using 300x and 250x magnification under a low-vacuum with a pressure of 0.974 torr, a voltage of 10kV, and a spot size of 4.0. Etiolated hypocotyl cells of five day old seedlings were viewed using 200x and 400x magnification under a high vacuum with a pressure of 0.0000198-0.0000495 torr, a voltage of 12.5kV, and a spot size of 3.0.

CHAPTER III

RESULTS AND DISCUSSION

GLH1

Identification of a Candidate Gene, *MED25*

GLH1 was previously fine mapped to an interval of 82 kilobases (kb) on the upper arm of chromosome 1, containing approximately twenty seven genes (Figure 5) (12). To pursue identification of this gene, eleven T-DNA lines that lie within this region were ordered from the Arabidopsis Biological Resource Center (http://abrc.osu.edu) and screened for a glassy trichome phenotype. Only one line, SALK_129555c, exhibited a glassy phenotype. The gene interrupted in this SALK line is *MED25*. A literature search revealed that *MED25* encodes a protein that functions as part of the transcription factor-interacting portion of a mediator complex (supplemental figure 1) (6). More specifically, MED25 has been shown to regulate jasmonate and abscisic acid signaling pathways through interacting with the MYC2 and ABI5 transcription factors. These signaling pathways play integral roles in mounting defensive and stress responses, such as to salt stress and fungal infections, and in controlling growth processes (27, 28). MED25 is also known to be involved in the regulation of flowering time in reaction to light quality, organ development through the restriction of cell proliferation and expansion, and repression of

Phytochrome B light signaling via interaction with the drought response element binding protein 2A (21, 29, 30). It has therefore been proposed that MED25 aids in the integration of signals from several different pathways, enabling the plant to respond appropriately to various stressors and developmental cues (29, 30). It follows then that such a gene may be involved in the development of trichomes, cells that are speculated to be protective in nature.

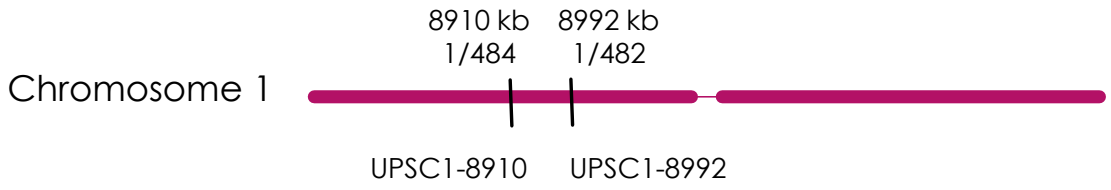

Figure 5 *GLH1* Mapping Interval

GLH1 was mapped to an 82kb region on chromosome 1. The names of the markers, their position on the chromosome, as well as the number of recombinants in relation to the number of chromosomes tested are all indicated.

Sequencing of *MED25*

In order to determine where exactly the causative mutation was located, *MED25* was PCR amplified in the mutant background and subsequently sequenced. An alignment with wild type Columbia sequences revealed that there was a point mutation at the beginning of the sixth intron that resulted in a Guanine to Adenine substitution. As the mutation is located within the exon-intron border, it is likely that it causes a splicing malfunction, possibly resulting in a truncated protein.

Complementation Testing

The SALK_129555c ("55c") line was then crossed with the *glh1* line to test for genetic complementation. Analysis of F1 trichome phenotype revealed that progeny possessed glassy trichomes, which indicates that the *med25* and *glh1* mutations are in the same gene (Figure 6). The pPZP212 vector containing a genomic fragment including the *MED25* regulatory and coding regions was also transformed into mutant plants to confirm gene identity. (The construct used for this transformation was obtained from Dr. Pablo Cerdan at La Universidad de Buenos Aires, Argentina.) The T1 generation was screened, and trichomes were found to exhibit a frosted phenotype (Figure 7). This indicates that the functional copy of *MED25* successfully rescued the mutant phenotype. This in turn, indicates that the *glh1* mutation is the *MED25* loss-of-function allele, and supports the results from the genetic cross.

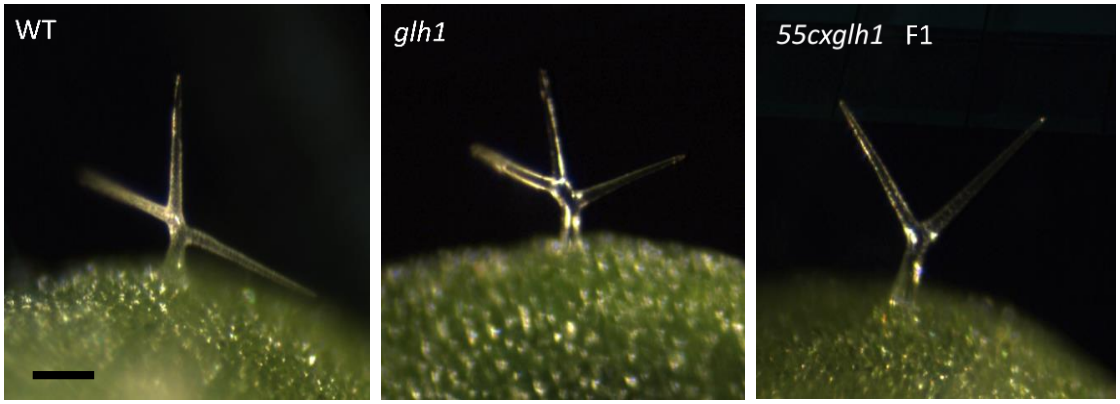

Figure 6 *glh1* Genetic Cross to Test Complementation

A cross between the *glh1* mutant and the SALK_12955C ("55c") line yielded glassy progeny. Wild type (left) plants possess trichomes with a frosted appearance. *glh1* (center) and *55cxglh1* F1 (right) plants both exhibit glassy trichomes. Scale bar=150µm.

Figure 7 *glh1* Mutant Rescue to Test Complementation

A functional copy of *MED25* was transformed into *glh1* mutants, producing wild type T1 trichomes. Wild type (left) and *MED25*pro:*MED25* T1 (right) plants both possess trichomes with a frosted appearance. *glh1* (center) plants exhibit glassy trichomes. Scale bar=150μm.

Expression of Trichome Developmental Markers

In addition, β-glucuronidase (GUS) fused markers for trichome development, *GLABRA2* (*GL2*) and *ETHYLENE RECEPTOR2* (*ETR2*), were genetically introduced into the mutant line. *GL2* is important for several stages of trichome development, including cell expansion, branching, and cell wall maturation. *GL2* is therefore expressed in both young and mature trichomes (31). *ETR2*, on the other hand, is important mainly in the early stages of trichome development involving microtubule array stabilization and branch formation. Accordingly, *ETR2* expression is highest in young trichomes (32). These specific markers were used to determine whether or not the *glh1* mutant phenotype resulted from general developmental arrest.

The F3 generations of the *glh1xGL2-GUS* and *glh1xETR2-GUS* crosses, along with the parental GUS lines were stained for GUS expression levels. No apparent discrepancy in GUS expression between the parental GUS and mutant lines were detected

(Figure 8). This indicates that the transcription of genes in trichomes is not generally changed in mutants, and that the *glh1* mutant phenotype is not the result of general developmental arrest. Consequently, this would suggest that *GLH1* has a more specific function involving papillae development.

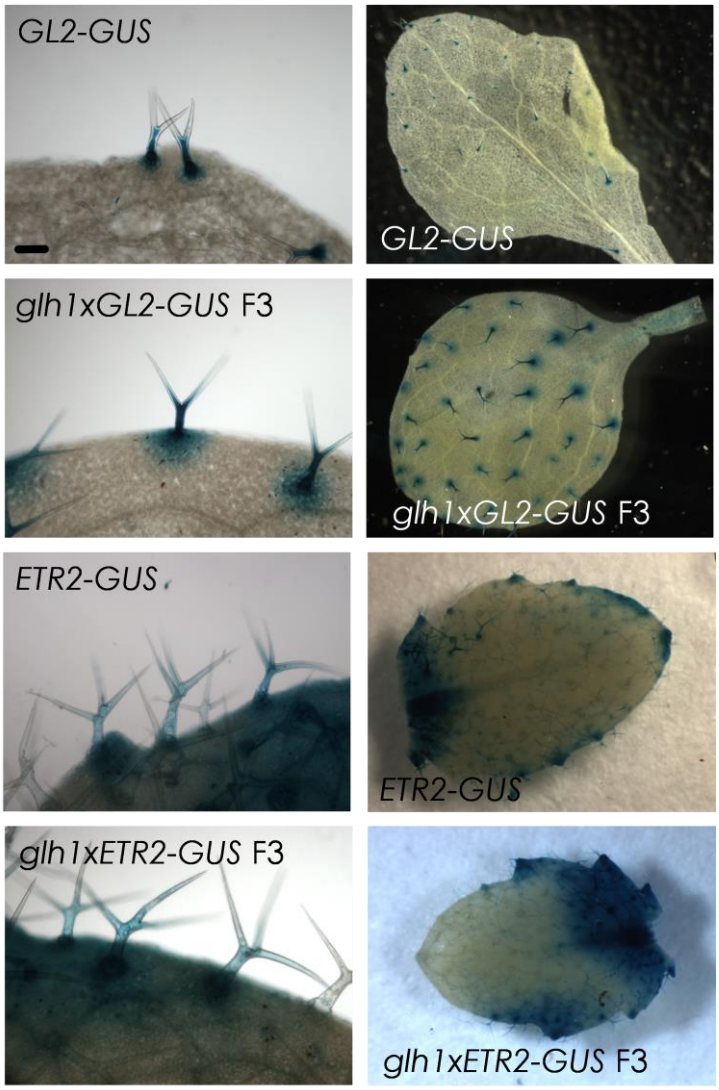

Figure 8 *GL2-GUS* and *ETR2-GUS* Expression in *glh1* Trichomes

No substantial difference in GUS expression between parental (wild type) and mutant plants was detected. Trichome (left column) and whole leaf (right column) images are shown for each parental and F3 line. Scale bar for trichome images=100µm.

MED25 Localization

Finally, the promoter of *MED25* was cloned into the pMDC162 vector to create a *MED25pro*:*GUS* fusion. This construct was transformed into Columbia wild type

plants, and the T1 generation was stained for GUS to determine the localization and relative levels of gene expression. GUS expression was seen primarily in leaf vasculature, guard cells, roots, tissue at the base of mature trichomes located at certain points on the leaf edge, developing trichomes, and trichomes of young leaves (Figure 9). Faint to semi-strong staining of trichomes on older leaves was also observed, particularly in lines exhibiting overall higher levels of GUS expression. Extremely young leaves tended to exhibit higher levels of GUS staining compared to that of older leaves. The detected expression profile is consistent with that previously described by Xu and Li 2011 (21), with the exception that they reported slightly higher GUS expression in older leaves compared to younger leaves, and GUS expression in trichomes was not examined. The discrepancy in GUS expression observed in younger versus older leaves may have resulted from the relatively short stain incubation time of two hours used in Xu and Li 2011 (21) in comparison with the overnight incubation used here.

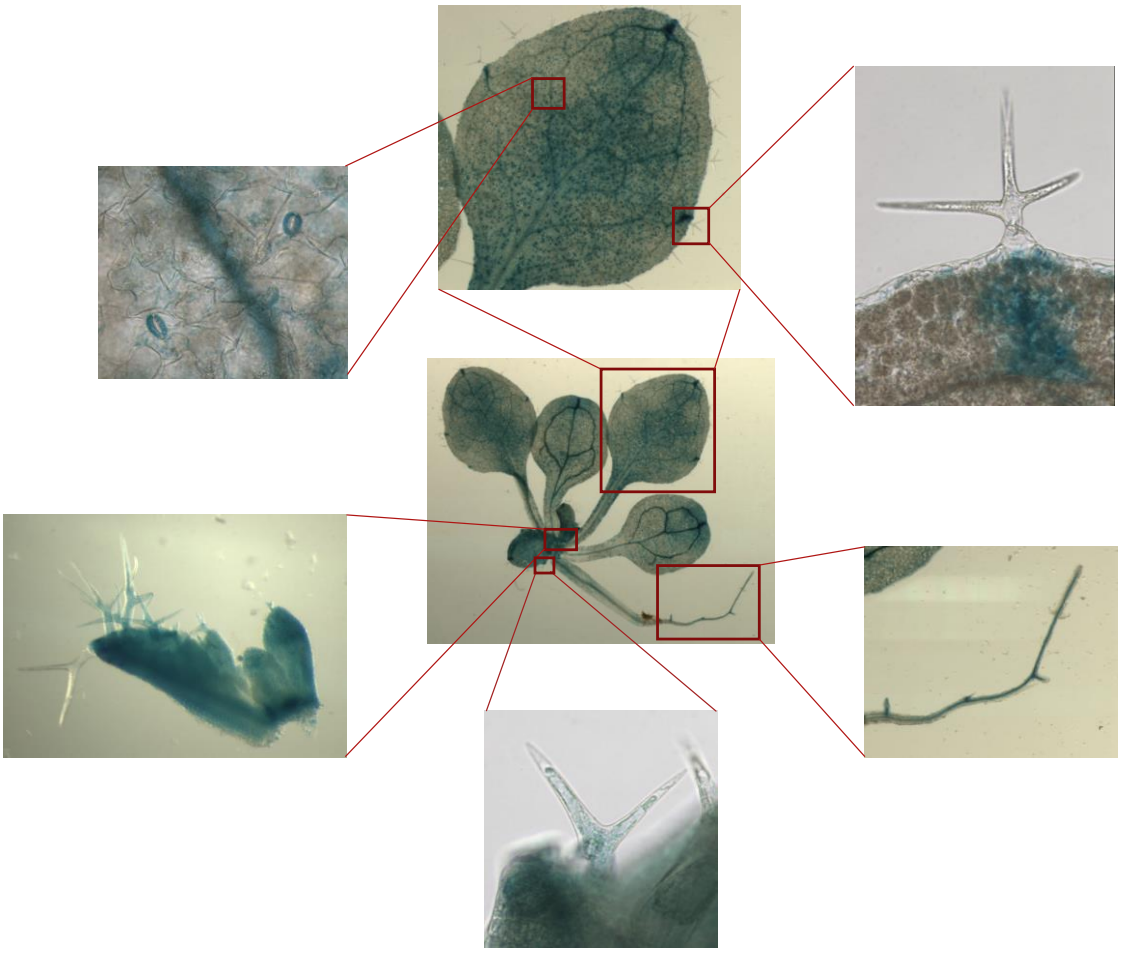

Figure 9 GUS Expression in *MED25pro:GUS* T3 Seedlings

GUS expression in ten-day-old seedlings was evident primarily in leaf vasculature, guard cells, roots, tissue at the base of mature trichomes located at certain points on the leaf edge, developing trichomes, and trichomes of young leaves.

Future Directions

The presence of GUS expression in leaf trichomes suggests that the *glh1* mutant phenotype may be a direct effect of the gene mutation. It follows then that *MED25* may directly interact with transcription factors necessary for the activation of genes involved in the localized deposition of material on the cell wall surface. In mutant plants

these genes would therefore not be transcribed, and papillae would be absent on the trichome cell wall surface. A transcriptome analysis using RNA isolated from wild type and mutant trichomes could be performed in the future to reveal genes that are differentially expressed in mutant versus wild type trichomes (33). This would allow for the identification of potential GLH1 interacting proteins, which may then be furthered studied to shed light on the exact mechanism by which *GLH1* is important for papillae deposition on the cell wall surface.

Higher GUS levels in very young leaves and developing trichomes suggest that *MED25* expression, and consequently the presence of papillae, may be important during early leaf developmental stages. It has been previously demonstrated that UV-B radiation hinders growth and development in *Arabidopsis*, causing decreases in rosette diameter, leaf size, stem heights, and delays in flowering time. Leaf trichomes, however were shown to provide some protection against these detrimental effects. Though it has been proven that UV-B absorbing compounds accumulate in trichomes, it has not yet been identified where exactly these protective compounds are located (2, 3). As a result, it is possible that these UV-B absorbing compounds lie in trichome papillae. To test this idea, *glh1* mutant trichomes and Columbia wild type trichomes were harvested. The absorbance of these trichomes will be measured at 305nm (the wavelength of UV-B radiation ranges from approximately 320-290nm). If a significant difference in the absorbance data is found between mutant and wild type trichomes, this would suggest that trichome papillae may function to protect developing leaf tissue from harmful UV-B damage. However, additional analysis of papillae composition would be needed to confirm this possibility.

GLH2

Mapping of *GLH2*

GLH2 had previously been rough mapped to a region near the centromere of chromosome 4 (Figure 10) (12). Additional mapping population samples were harvested and have been stored in the -80°C freezer. DNA can be isolated from these samples in the future, and used to decrease the fine mapping interval to approximately 100kb.

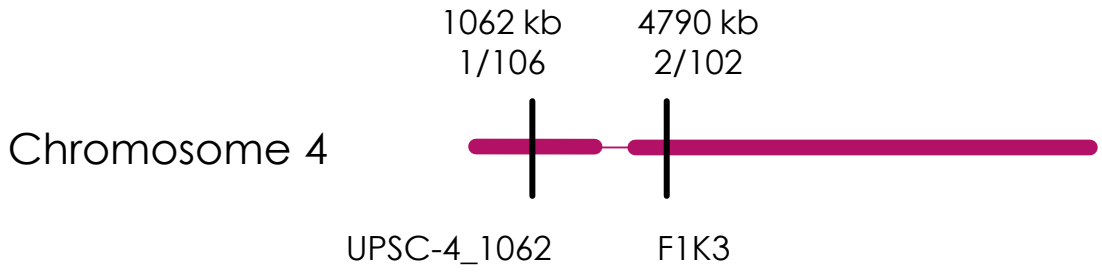

Figure 10 *GLH2* Mapping Interval

GLH2 was mapped to a 3,728kb region on chromosome 4. The names of the markers, their position on the chromosome, as well as the number of recombinants in relation to the number of chromosomes tested are all indicated.

Expression of a Trichome Developmental Marker

To further this project and begin characterizing the *glh2* mutation, GUS fused markers for trichome development, *GLABRA2* (*GL2*) and *ETHYLENE RECEPTOR2* (*ETR2*), were crossed into the mutant line. While mutant crosses with *ETR2-GUS* were unsuccessful, crosses with *GL2-GUS* were fruitful. The F3 generation of the *glh2xGL2-GUS* cross, along with the *GL2-GUS* parental line, were stained for GUS expression. No apparent difference in GUS expression between the parental GUS line and the F3 generation were detected (Figure 11). As with *glh1*, this shows that the transcription of genes in trichomes is not generally changed in *glh2* mutants. The *glh2* mutant phenotype

is thus not the result of general developmental arrest. Which would suggest that *GLH2* has a more specific function involving papillae development.

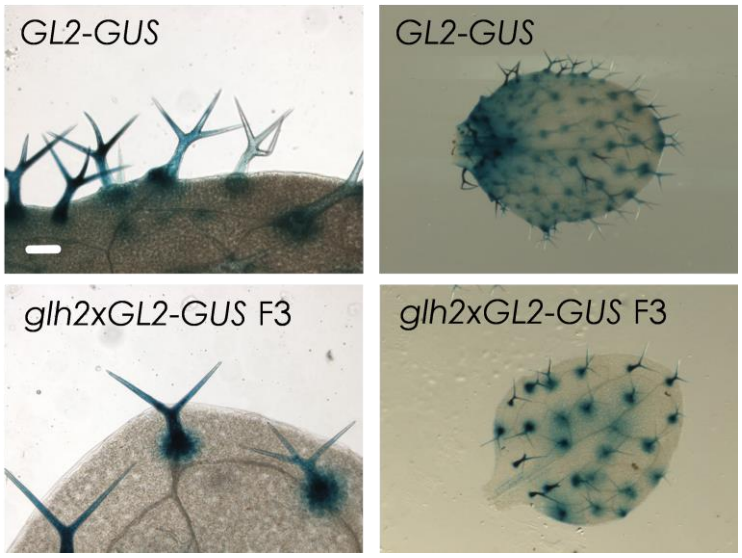

Figure 11 *GL2-GUS* Expression in *glh2* Trichomes

No substantial difference in GUS expression between parental (wild type) and mutant plants was detected. Trichome (left column) and whole leaf (right column) images are shown for each parental and F3 line. Scale bar for trichome images=100µm.

Sequencing *MED21*, a Candidate Gene for *glh2*

Since *glh2* exhibited a similar phenotype as *glh1*, and the genetic analysis using developmental markers also yielded comparable results, the chance that a mediator gene was also responsible for the *glh2* mutation was considered. To investigate this possibility, the mapping interval for *GLH2* was screened for known mediator subunit genes. The search returned one such gene, *MED21*. According to the literature, MED21 is involved in the regulation of developmental and defense pathways, like MED25. More specifically, MED21 is known to be required for embryo development and is involved in mounting defense responses against fungal pathogens (34).

To test the gene identity of *MED21* as *GLH2*, *MED21* was PCR amplified in the mutant background and subsequently sequenced. An alignment with wild type

Columbia sequences revealed that *glh2* mutants did not contain a mutation site within this gene. This indicates that *MED21* is not *GLH2*, and that a different gene must be responsible for the *glh2* phenotype.

Future Directions

In the future, additional mapping and the reduction of the mapping interval for *GLH2* will be needed. Once the mapping interval is reduced to under 100kb, T-DNA lines disrupting genes within that interval may be ordered and screened for a glassy phenotype. After a candidate gene is located, then sequencing analysis and complementation testing may be performed to confirm gene identity.

GLH3

Mapping of *GLH3*

GLH3 was previously rough mapped to a region on the lower arm of chromosome 5 (12). Recent mapping efforts have reduced the mapping interval from approximately 2,000kb to 367kb (Figure 12). Additional mapping population samples were also harvested and have been stored in the -80^{o}C freezer. DNA can be isolated from these samples in the future, and used to decrease the fine mapping interval to approximately 100kb.

Figure 12 *GLH3* Mapping Interval

GLH3 was mapped to a 367kb region on chromosome 5. The names of the markers, their position on the chromosome, as well as the number of recombinants in relation to the number of chromosomes tested are all indicated.

Future Directions

Initial characterization of the *glh3* mutation was begun by introducing GUS fused markers for trichome development, *GLABRA2* (*GL2*) and *ETHYLENE RECEPTOR2* (*ETR2*), into the mutant line. Seeds from the F1 generation were harvested and planted. Seeds from these F2 plants will also need to be collected and planted so that the F3 generation may be analyzed for GUS expression in the future. Such an analysis would reveal whether the *glh3* mutation is the product of general developmental arrest, or if *GLH3* has a more specific function in the papillae development pathway.

As with *GH2*, additional mapping will be necessary in the future to decrease the mapping interval for *GLH2* to approximately 100kb. Once that is achieved, T-DNA lines disrupting genes within that interval may be ordered and screened for a glassy phenotype. After a candidate gene is located, then sequencing analysis and complementation testing may be performed to confirm gene identity.

SH

Mapping of *SH*

The *SH* gene had been previously discovered segregating out of the *glh2* mapping population. To begin investigating this mutation, genetic mapping was recently carried out to determine the location of the *SH* gene. *SH* was subsequently rough mapped to a 2,791kb region on the lower arm of chromosome 5 (Figure 13). Phenotyping of *sh* mutants segregating out of the mapping population proved difficult due to natural variation in the hypocotyl length of dark grown Colombia wild type plants. As a result, the mutant phenotype was verified in the next generation, and any lines exhibiting an intermediate or wild type hypocotyl phenotype were discarded.

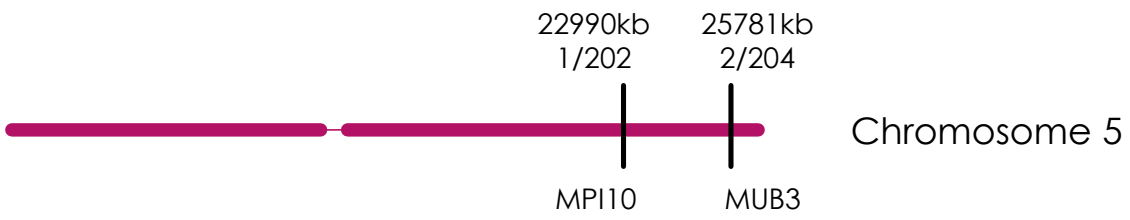

Figure 13 *SH* Mapping Interval

SH was mapped to a 2,791kb region on chromosome 5. The names of the markers, their position on the chromosome, as well as the number of recombinants in relation to the number of chromosomes tested are all indicated.

sh-like Mutants

Since many mutations that result in a short hypocotyl phenotype have been previously described (13-17), the mapping interval was searched for known mutants that have *sh*-like phenotypes. Two such mutants were found: *cobra(cob)* and *procuste(prc)*. *COBRA* encodes a glycosyl-phosphatidyl inositol-anchored protein that regulates anisotropic cell expansion through its involvement in the oriented deposition of cellulose

microfibrils. Mutants lacking COBRA are deficient in hypocotyl elongation when grown in darkness, and exhibit conditional radial expansion (CORE) of the roots, hypocotyl, and cotyledons when grown on high sucrose media (17). *PROCUSTE* encodes cellulose synthase 6, or CESA6, a subunit of the cellulose synthase complex involved in primary cell wall cellulose synthesis. The *prc/cesa6* mutant phenotype is characterized by reduced elongation in roots and the hypocotyls of dark-grown plants (15).

Conditional Radial Expansion Test: *SH* is not *COBRA*

To ensure that *SH* was a novel gene and not, in fact, *COB* or *PRC*, a variety of analyses were performed. A conditional radial expansion test, involving the growth of plants on high and low sucrose media, was conducted to determine whether or not *sh* mutants exhibited a CORE phenotype consistent with that seen in *cobra* mutants (see methods section for additional details concerning experimental conditions) (17). Although the *sh* phenotype was more distinct when high sucrose conditions were used, radial swelling was not observed (Figure 14). This indicates that unlike *cobra* mutants, *short hypocotyl* mutants do not exhibit conditional radial expansion when exposed to high levels of sucrose, and it is unlikely that *SH* and *COB* are the same gene. However, a cross between *sh* and *cobra* should be conducted in the future to test complementation and confirm this result.

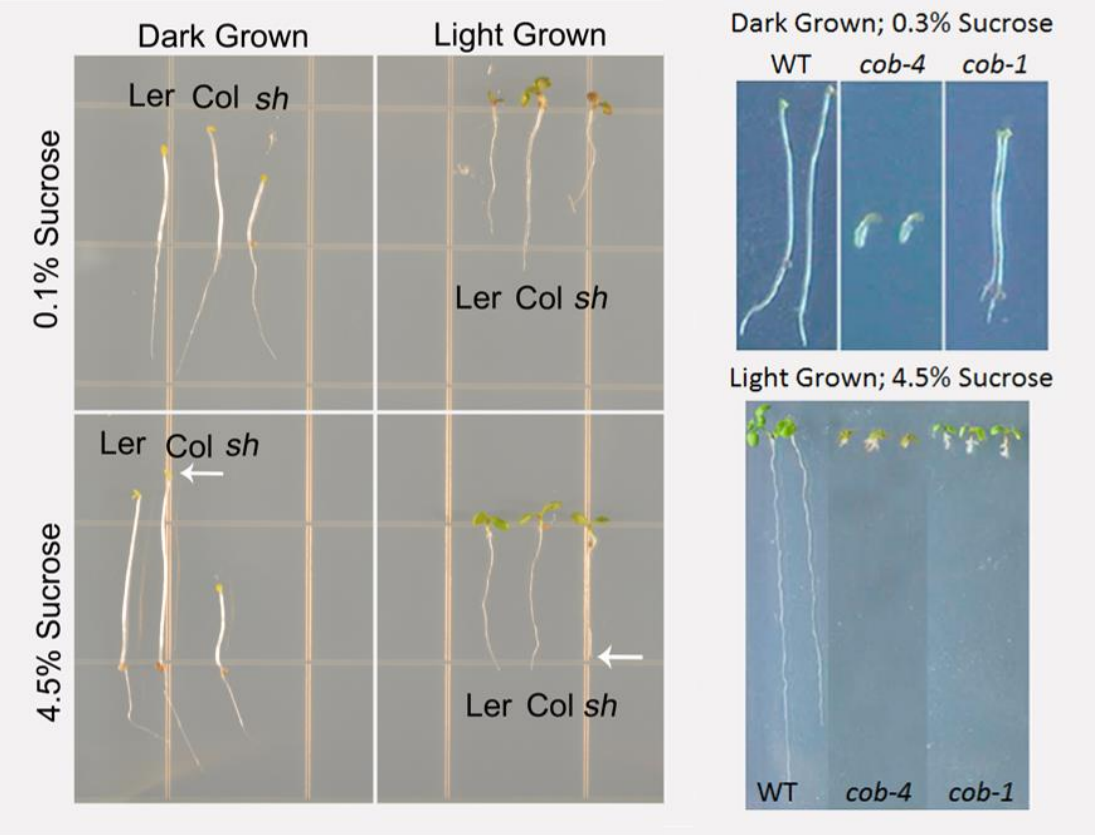

Figure 14 Conditional Radial Expansion Test

Lansberg (Ler), Colombia (Col), and *short hypocotyl* plants were grown under one of four sets of conditions (left): 1. in darkness and on 0.1% sucrose, 2. in darkness and on 4.5% sucrose, 3. in light and on 0.1% sucrose, 4. in light and on 4.5% sucrose. Colombia, *cobra-4*, and *cobra-1* plants were grown under one of two sets of conditions (right): 1. in darkness and on 0.3% sucrose, 2. in light and on 4.5% sucrose. Unlike *cobra* mutants, *short hypocotyl* mutants do not exhibit conditional radial expansion when grown under high sucrose conditions. Right images reproduced with permission from Roudier *et al* 2005 (17).

Confocal Microscopy and a Genetic Cross: *SH* is not *PRC*

In addition, a confocal microscopy analysis of progeny from a *sh* x YFP-tagged CESA6 cross was completed as a way to test complementation as well as to visualize CESA6 expression at the plasma membrane of Colombia wild type and mutant plants.

Progeny from the cross still demonstrated short hypocotyls, indicating that the functional copy of *CESA6* failed to rescue the mutant phenotype. An independent cross of the *prc* line with *sh* plants yielded wild type progeny (Figure 15). Together these results suggest that *SH* and *PRC/CESA6* are not the same gene. However, confocal imaging and subsequent quantitative analysis revealed that CESA6 particle density at the plasma membrane in mutant plants is reduced to 43.25% of wild type levels (Figure16). Quantification of CESA6 particle density was performed according to the protocol used by Bashline *et al.* 2013 (26).

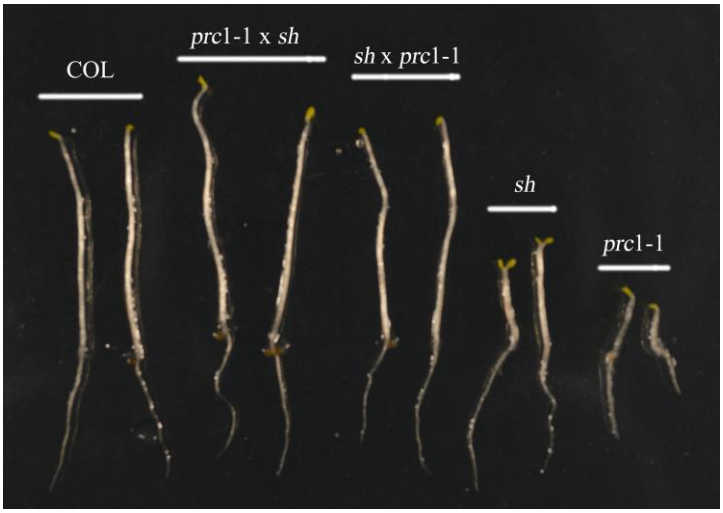

Figure 15 *sh* Genetic Cross to Test Complementation

sh was crossed with *prc*, to test genetic complementation. The cross was performed in duplicate, with both lines serving as mother plants. The mother plant line was listed first when naming the F1 generations. Wild type progeny indicates that the *sh* and *prc* mutations are not in the same gene.

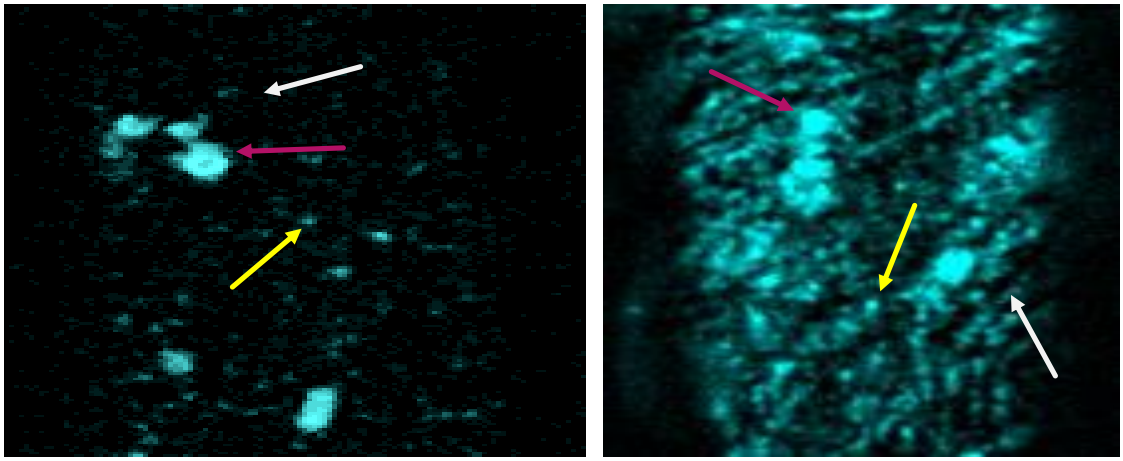

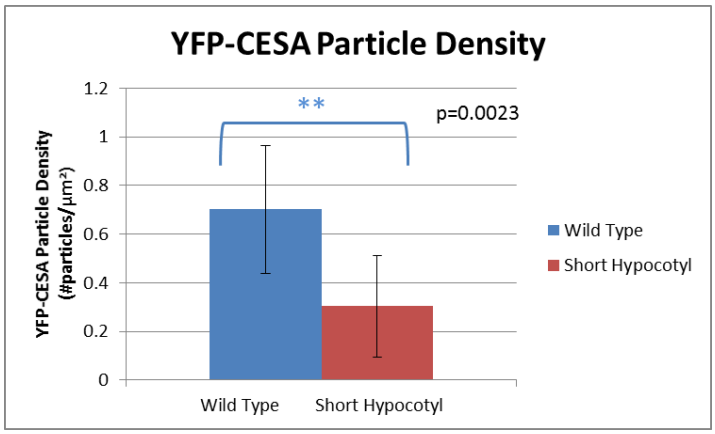

Figure 16 *sh* x YFP-CESA6

YFP-CESA6 particle density at the plasma membrane in *sh* mutants is reduced to 43.25% of wild type levels. White arrows indicate individual CESA6 particles, magenta arrows indicate Golgi, and yellow arrows indicate SmaCCs. ** indicates a highly significant p value. n=11 for *sh*, and n=10 for wild type measurements. Error bars represent standard deviation.

Future Directions Part One

Individual CESA subunits are most likely produced in the endoplasmic reticulum, but it is believed that they are assembled into cellulose synthase complexes (CSCs) in plant

Golgi before being transported to the plasma membrane. This is because the Golgi apparatus is the earliest stage in the endomembrane system where CSCs have been detected (35). While measuring CESA6 particle density, it was also observed that CESA6 signal intensity appears to be higher in the Golgi apparatuses of mutants. This suggests that CESA6 may be sequestered in Golgi of *sh* plants. It is possible, however, that the decrease in CESA6 particle density at the plasma membrane is merely causing Golgi signal to become more visible. A quantitative analysis of CESA6 signal intensity in the Golgi of wild type and mutant plants will be required to determine whether CESA6 is actually accumulating in Golgi of mutant plants.

Taken together, the above observations and data indicate that *sh* may be a vesicle trafficking mutant. If this is the case, in addition to measuring Golgi signal intensity, the signal intensity and density of small CESA compartments (SmaCCs) should also be measured. SmaCCs are believed to be involved in the delivery and/or internalization of CESAs to/from the plasma membrane (35, 36). Therefore, the comparison of SmaCC CESA6 signal intensity and density in mutants to wild type values could potentially shed light on which step in the CESA trafficking process is affected by the *sh* mutation.

Birefringence Analysis

Since CESA6 particle density at the plasma membrane was reduced in *sh* mutants, steps were also taken to determine if a consequential cellulose deficiency existed in mutant plants. Birefringence, an optical property of crystalline cellulose, is caused by the conditional refractive index of this cell wall material. The parallel and perpendicular polarized component waves of an incident beam of light are refracted, or bent, at slightly

different angles in substances rich in crystalline cellulose, causing the beam to be split and double refraction of the light to occur. Polarized light microscopy was used to achieve maximum birefringence of single *sh* and wild type trichome branches (25). The relative light intensity of these branches was measured as a way to quantify birefringence and to determine if cellulose content was potentially altered in mutants. Significantly lower light intensity was measured in mutant trichomes (70.24% of that of wild type), suggesting a possible cellulose deficiency in *sh* mutants (Figure 17).

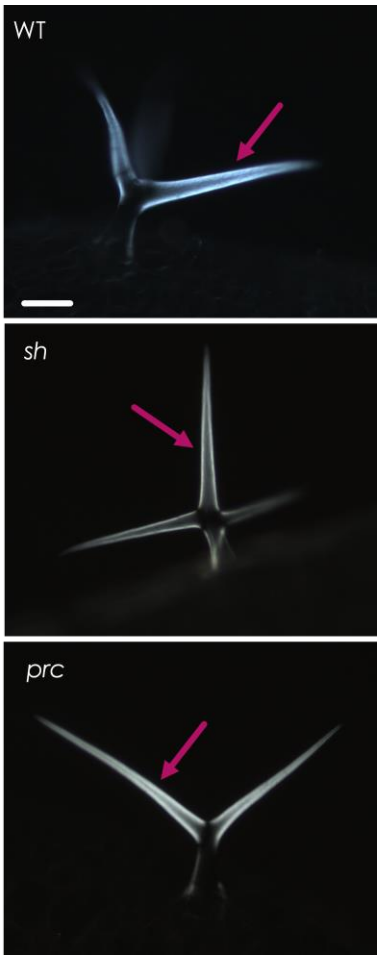

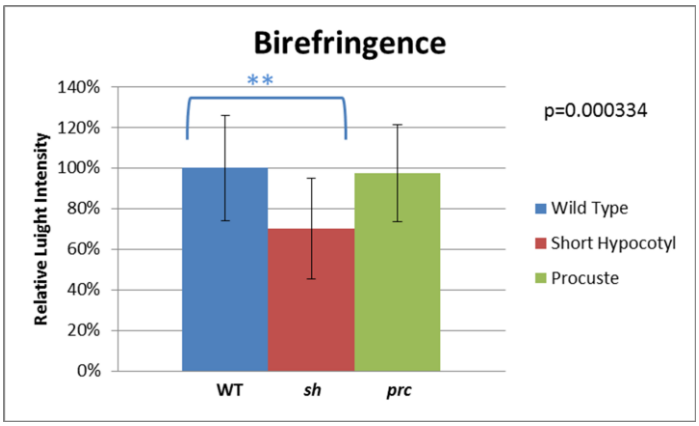

Figure 17 Trichome Birefringence

Wild type, *sh*, and *prc* trichomes displaying maximum birefringence. *sh* trichomes only yield 70.24% of the relative light intensity that wild type trichomes are able to produce under maximum birefringence conditions. Arrows indicate branches for which light intensity was measured. Scale bar = 75µm. ** indicates a highly significant p value. n=20 for wild type and *sh* measurements. n=22 for *prc* measurements. Error bars represent standard deviation.

Cellulose Quantification

To test the possibility of a cellulose reduction in *sh* plants, a colorimetric biochemical anthrone assay was used to quantify the cellulose content of five-day-old dark-grown wild type, *sh*, and *prc* seedlings (23, 24). *prc* mutants have been previously shown to have a cellulose deficiency, and so they were included as a positive control (15). Though an approximate 9% reduction in cellulose levels of *sh* seedlings was seen, it was not a statistically significant difference (Figure 18). The *prc* mutants, on the other hand showed a statistically significant cellulose reduction of about 46%, which is consistent with previously reported values (15).

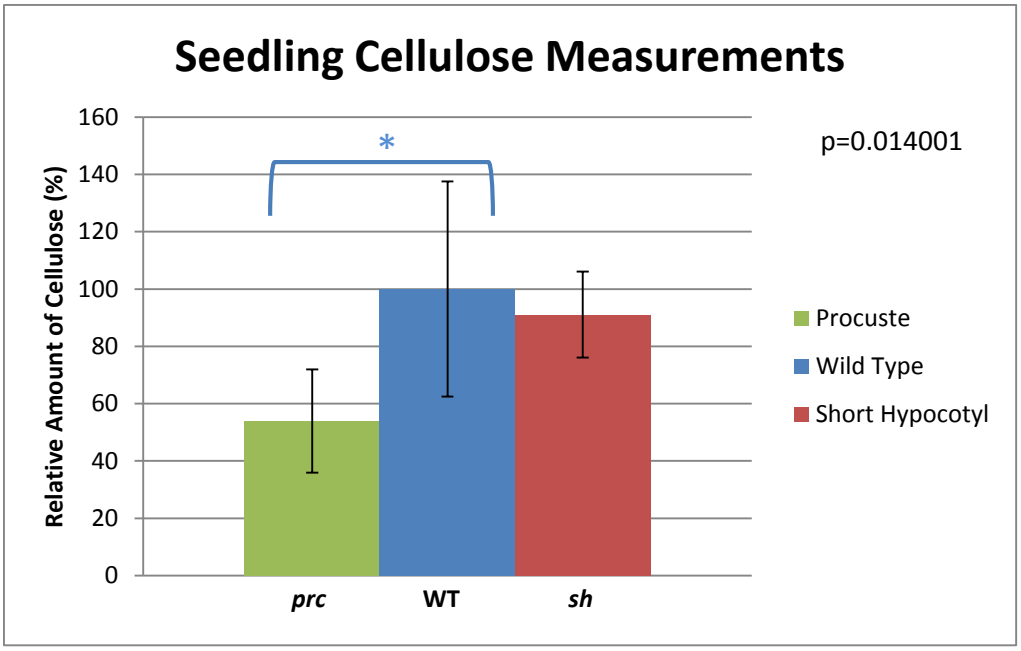

Figure 18 Mutant Seedling Cellulose Content Relative to Wild Type Levels
In comparison to wild type, *sh* and *prc* mutants exhibited 8.96% and 46.08% less cellulose, respectively. * indicates a significant p value. n=12 for *prc*, n=10 for *sh*, and n=7 for wild type measurements. Error bars represent standard deviation.

It is possible that the discrepancy seen between the confocal microscopy, birefringence, and cellulose quantification data could be due to the unusual nature of the

trichome cell wall. Since CESA6 is involved in primary cell wall synthesis, it is logical to think that a mutation affecting its (and likely the whole primary CSC's) transportation to the plasma membrane would result in a cellulose deficiency in the primary cell wall (15, 36, 37). However, cellulose measurements of whole seedlings included both primary and secondary cell wall materials. Secondary cell walls have higher cellulose content than primary cell walls, and assuming the *sh* mutation does not affect the trafficking of secondary CESAs and CSCs, this might be masking any deficiency in primary cell wall cellulose (25, 36, 37). The cell walls of *Arabidopsis* trichomes, though they are very thick, more closely resemble primary cell walls. This could be a result of the lack of secondary CESAs and involvement of primary CESAs in cell expansion and secondary wall thickening in trichomes (18, 22, 36). A problem in primary cell wall synthesis, therefore, would likely be more noticeable in trichomes. Such a difference may not have been seen in the birefringence data for the *prc* mutant because the plants used for birefringence analysis were grown in light conditions. As it has been previously shown, light restores normal growth and cellulose synthesis in *cesa6* mutants. This is due to the induction of the *PRC1*-independent elongation growth program and the override of CSC velocity inhibition by Phytochrome B (38, 39). As a result, light-grown *cesa6* trichomes would be expected to display wild type levels of birefringence.

To test the concept that the less birefringent *sh* trichomes may exhibit a corresponding decrease in cellulose, the cellulose content of mutant and wild type trichomes was measured using the same anthrone biochemical assay used for seedling measurements. The assay results indicated that cellulose levels were decreased by 57.92% in *sh* trichomes in comparison to wild type levels (Figure 19).

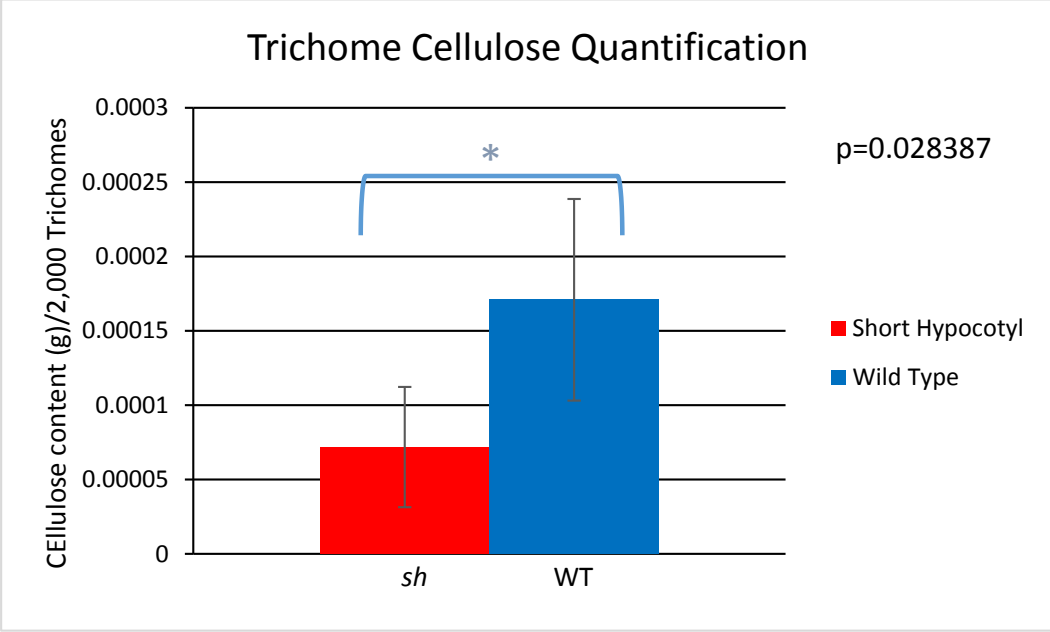

Figure 19 Cellulose Content of Trichomes
The cellulose content in 2,000 *sh* trichomes was 57.92% less than that found in the same number of wild type trichomes. * indicates a significant p value. n=5 for both wild type and *sh* measurements. Error bars represent standard deviation.

Future Directions Part Two

Alternatively, the altered level of cellulose in the trichomes of *sh* mutants may be independent of the CESA6 phenotype observed in the hypocotyls. It is possible that the lack of a detected cellulose deficiency is due to prolonged lifetime or increased productivity of primary CSCs that make it to the plasma membrane. The dwarfed phenotype of dark-grown hypocotyls could also be explained by altered levels of methylesterfied pectins, for example, and does not necessary have to be linked to a decrease in crystalline cellulose. Such is the case in the *trichome birefringence* mutant, where a decrease in cellulose was seen in trichomes but not in the hypocotyl (25).

Additional testing of cell wall composition and primary CSC activity will be needed to address these areas of inquiry.

CHAPTER IV

CONCLUSIONS

Cells walls are versatile structures, important for several aspects of plant survival. While many processes of cell wall biogenesis have been studied, there is still much left to learn. The research presented here is a step in that direction. For instance, *GLH1*, a gene important leaf trichome papillae deposition on the cell wall surface, has been identified as *MED25*. Characterization of the *glh1* mutation has made it clear that this mediator complex subunit has a specific role in trichome maturation, but the details by which this is accomplished are still unknown. To provide insight on this subject, a transcriptome analysis of genes expressed in wild type and mutant trichomes could be performed in the future to isolate GLH1 interacting proteins.

Mapping and preliminary characterization of two additional genes important for trichome papillae development, *GLH2* and *GLH3*, have also been performed. At least one of these genes has been shown to have a specific role in trichome cell wall development, but appears to contribute to papillae deposition differently than *GLH1*. The identification and characterization of these genes may therefore provide additional information regarding the complicated process that leads to the localized deposition of material on the trichome cell wall.

In addition, *SH* has thus far been shown to be a novel gene important for cell elongation in dark-grown hypocotyls. Dark-grown mutants demonstrate reduced CESA6 particle density at the plasma membrane, which may be the result of a trafficking defect. Cellulose analysis indicates that the gene is also important for cellulose deposition in the trichome cell wall. Further analysis of CESA6 signal intensity and density, as well as additional characterization of cell wall composition could shed light on the precise function of this gene.

Though several mutations have been identified that cause a short hypocotyl or glassy trichomes, most of these mutations target distinct players in the cell wall biogenesis and developmental pathways. Through the identification and characterization of the *GLH* and *SH* genes, we may gain insight into the complex molecular and cellular pathways involved in cell wall biogenesis, the deposition of materials on the cell wall surface, and oriented cell expansion.

REFERENCES

1. P. Dalin, J. Agren, C. Bjorkman, *et al*. *Induced Plant Resistance to Herbivory*. A. Schaller, Ed. (Springer, Berlin, 2008), chap. 4, pp. 89-105.

2. Karabourniotis, Kotsabassidis, and Manetas. Trichome density and its protective potential against ultraviolet-B radiation-damage during leaf development. *Canadian Journal of Botany*. 75(3): 376-383 (1995).

3. A.Yan, J. Pan, L. An, *et al*. The responses of trichome mutants to enhanced ultraviolet-B radiation in *Arabidopsis thaliana*. *Journal of Photochemistry and Photobiology B: Biology*. 113: 29-35 (2012).

4. G. Refregier, S. Pelletier, D. Jaillard, *et al*. Interaction between wall deposition and cell elongation in dark-grown hypocotyl cells in *Arabidopsis*. *Plant Physiology*. 135: 959-968 (2004).

5. D. Meinke, J. Cherry, C. Dean, *et al. Arabidopsis thaliana:* a model plant for genome analysis. *Science.* 282: 662-682 (1998).

6. S. Backstrom, N. Elfving, R. Nilsson, *et al.* Purification of a plant mediator from *Arabidopsis thaliana* identifies PFT1 as the MED25 subunit. *Molecular Cell.* 26: 717-729 (2007).

7. R. Hatfield, J. Ralph, J. Grabber. Cell wall cross-linking by ferulates and diferulates in grasses. *Journal of the Science of Food and Agriculture.* 79: 403-407 (1999).

8. P. Albersheim, A. Darvill, C. Augur, *et al*. Oligosaccharins: oligosaccharide regulatory molecules. *Accounts of Chemical Research*. 25(2): 77-83 (1992).

9. T. Baskin. Anisotropic expansion of the plant cell wall. *Cell and Developmental Biology*. 21: 203-222 (2005).

10. G. Gutierrez-Alcala, C. Gotor, A. Meyer, *et al.* Glutathione biosynthesis in *Arabidopsis* trichome cells. *PNAS.* 97(20): 11108-11113 (2000).

11. J. Dominguez-Solis, M. Lopez-Martin, F. Ager, *et al.* Increased cysteine availability is essential for cadmium tolerance and accumulation in *Arabidopsis thaliana. Plant Biotechnology Journal.* 2: 469-476 (2004).

12. B. Suo, S. Seifert, and V. Kirik. *Arabidopsis GLASSY HAIR* Genes Promote Trichome Papillae Development. *Journal of Experimental Botany*. 64(16): 4981-4991 (2013).

13. S. Sato, T. Kato, K. Kakegawa, *et al.* Role of the putative membrane-bound endo-1,4-β-glucanase KORRIGAN in Cell Elongation and Cellulose Synthesis in *Arabidopsis thaliana. Plant Cell Physiology.* 42(3): 251-263 (2001).

14. S. Bosca, C. Barton, N. Taylor, *et al.* Interactions between *MUR10/CESA7*-dependent secondary cellulose biosynthesis and primary cell wall structure. *Plant Physiology.* 142: 1353-1363 (2006).

15. M. Fagard, T. Desnos, T. Desperez, *et al. PROCUSTE1* encodes a cellulose synthase required for normal cell elongation specifically in roots and dark-grown hypocotyls of *Arabidopsis*. *The Plant Cell.* 12: 2409-2423 (2000).

16. S. Pagant, A. Bichet, K. Sugimoto, *et al. KOBITO1* encodes a novel plasma membrane protein necessary for normal synthesis of cellulose during cell expansion in *Arabidopsis. The Plant Cell.* 14: 2001-2013 (2002).

17. F. Roudier, A. Fernandez, M. Fujita, *et al.* COBRA, an *Arabidopsis* extracellular glycosyl-phosphatidyl inositol-anchored protein, specifically controls highly anisotropic expansion through its involvement in cellulose microfibril orientation. *The Plant Cell*. 17: 1749–1763 (2005).

18. M. Jakoby, D. Falkenhan, M. Mader, *et al*. Transcriptional profiling of mature *Arabidopsis* trichomes reveals that *NOECK* encodes the MIXTA-like transcriptional regulator MYB106. *Plant Physiology*. 148: 1583-1602 (2008).

19. M. Hulskamp, S. Misera, and G. Jurgens. Genetic dissection of trichome cell development in *Arabidopsis*. *Cell.* 76: 555 – 566 (1994).

20. W. Lukowitz, C. Gillmor, W. Scheible. Positional cloning in *Arabidopsis*. Why it feels good to have a genome initiative working for you. *Plant Physiology.* 123: 795-805 (2000).

21. R. Xu, Y. Li. Control of final organ size by mediator complex subunit 25 in *Arabidopsis thaliana. Development.* 138: 4545-4554 (2011).

22. M. Marks, L. Betancur, E. Gilding, *et al*. A new method for isolating large quantities of *Arabidopsis* trichomes for transcriptome, cell wall and other types of analyses. *The Plant Journal.* 56: 483–492 (2008).

23. D. Updegraff. Semimicro determination of cellulose in biological materials. *Analytical Biochemistry*. 32 (3): 420–424 (1969).

24. C. Gillmor, P. Poindexter, J. Lorieau, *et al.* α-glucosidase I is required for cellulose biosynthesis and morphogenesis in *Arabidopsis. The Journal of Cell Biology.* 156(6): 1003-1013 (2002).

25. V. Bischoff, S. Nita, L. Neumetzler, *et al. TRICHOME BIREFRINGENCE* and its homolog AT5G01360 encode plant-specific DUF231 proteins required for cellulose biosynthesis in *Arabidopsis. Plant Physiology.* 153: 590-602 (2010).

26. L. Bashline, S. Li, C. Anderson, *et al.* The endocytosis of cellulose synthase in *Arabidopsis* is dependent on μ2, a clatherin-mediated endocytosis adaptin. *Plant Physiology.* 163: 150-160 (2013).

27. R. Chen, H. Jiang, L. Li, *et al.* The *Arabidopsis* mediator subunit MED25 differentially regulates jasmonate and abscisic acid signaling through interacting with the MYC2 and ABI5 transcription factors. *Plant Cell.* 24: 2898-2916 (2012).

28. B. Kidd, C. Edgar, K. Kumar, *et al.* The mediator complex subunit PFT1 is a key regulator of jasmonate-dependent defense in *Arabidopsis. The Plant Cell.* 21: 2237-2252 (2009).

29. S. Inigo, M. Alvarez, B. Strasser, *et al.* PFT1, the MED25 subunit of the plant mediator complex, promotes flowering through CONSTANS dependent and independent mechanisms in *Arabidopsis. The Plant Journal.* 69: 601-612 (2012).

30. N. Elfving, C. Davoine, R. Benlloch, *et al.* The *Arabidopsis thaliana* MED25 mediator subunit integrates environmental cues to control plant development. *PNAS.* 108(20): 8245-8250 (2011).

31. D. Szymanski, R. Jilk, S. Pollock, *et al.* Control of *GL2* expression in *Arabidopsis* leaves and trichomes. *Development.* 125: 1161-1171 (1998).

32. J. Plett, J. Mathur, S. Regan. Ethylene receptor ETR2 controls trichome branching by regulating microtubule assembly in *Arabidopsis thaliana. Journal of Experimental Botany.* 60(13): 3923-3933 (2009).

33. M. Marks, J, Wenger, E. Gilding, *et al.* Transcriptome analysis of *Arabidopsis* wild-type and *gl3–sst sim* trichomes identifies four additional genes required for trichome development. *Molecular plant.* 2(4): 803-822 (2009).

34. R. Dhawan, H. Luo, A. Foerster, *et al.* HISTONE MONOUBIQUITINATION1 interacts with a subunit of the mediator complex and regulates defense against necrotrophic fungal pathogens in *Arabidopsis. The Plant Cell.* 21: 1000-1019 (2009).

35. L. Bashline, S. Li, Y. Gu. The trafficking of the cellulose synthase complex in higher plants. *Annals of Botany.* 114(6):1059-1067 (2014).

36. L. Lei, S. Li, Y. Gu. Cellulose synthase complexes: composition and regulation. *Frontiers in Plant Science.* 3(75): 1-6 (2012).

37. L. Betancur, B. Singh, R. Rapp, *et al.* Phylogenetically distinct cellulose synthase genes support secondary cell wall thickening in *Arabidopsis* shoot trichomes and cotton fiber. *Journal of Integrative Plant Biology.* 52(2): 205-220 (2010).

38. T. Desnos, V. Orbovic, C. Bellini, *et al. Procuste1* mutants identify two distinct genetic pathways controlling hypocotyl cell elongation, respectively in dark- and light-grown *Arabidopsis* seedlings. *Development.* 122: 683-693 (1996).

39. V. Bischoff, T. Desprez, G. Mouille, *et al.* Phytochrome Regulation of Cellulose Synthesis in *Arabidopsis. Current Biology.* 21: 1822-1827 (2011).

APPENDIX A

SUPPLEMENTAL FIGURE

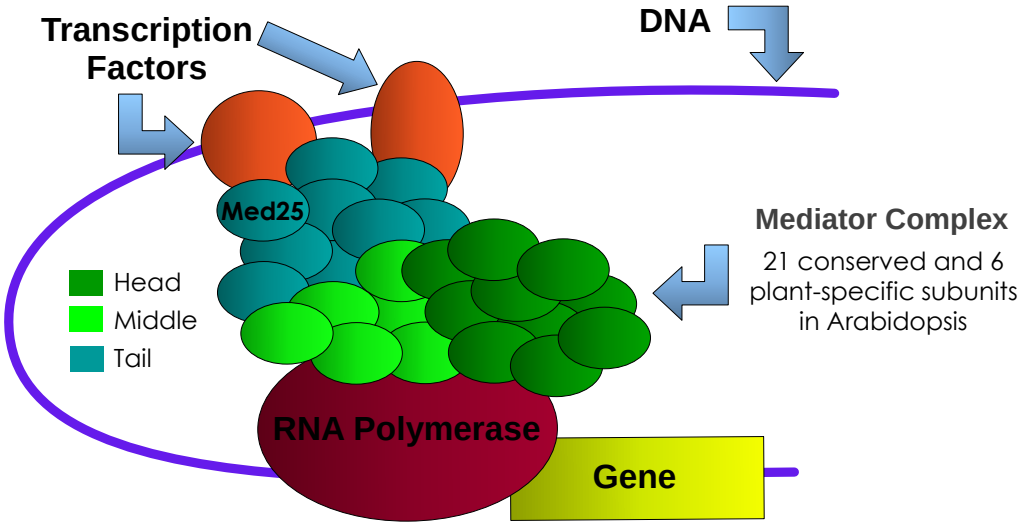

Supplemental Figure 1 MED25 is Part of a Mediator Complex

MED25 functions as part of the transcription factor-interacting portion of a mediator complex, aiding in the regulation of gene transcription.